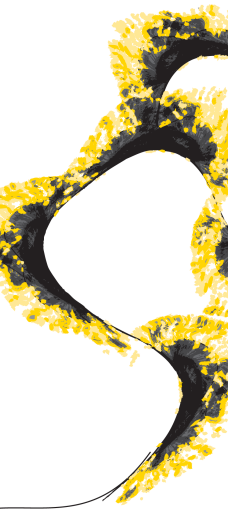

UNIVERSITY OF TWENTE.

Thesis Report

3D Weaving of Continuous Fiber Reinforced Soft Robot

Arman Goshtasbi, s2527197

Master's Thesis

20-04-2023

Document Number : BE-921

Department of Biomechanical Engineering
Faculty of Engineering Technology

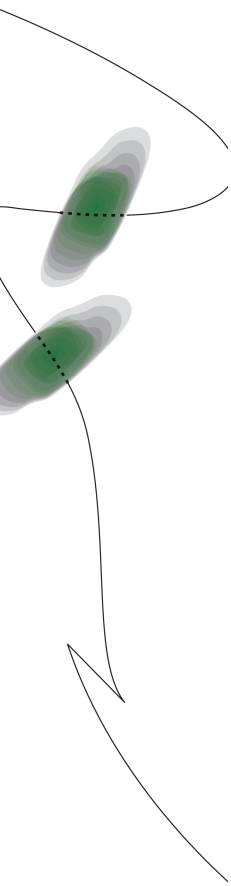

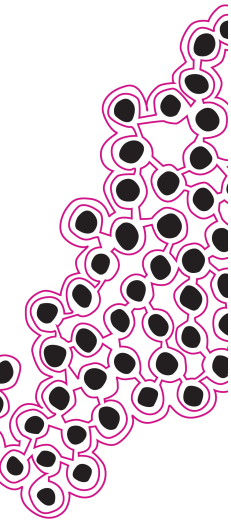

Graduation Committee
Prof. dr. ir Herman van der Kooij
Chairman
dr. Ali Sadeghi
Daily Supervisor
dr. Davoud Jafari
External Member

Biomechanical Engineering
Faculty of Engineering Technology
university of Twente
P.O. Box 217
7500 AR Enschede
The Netherlands

Abstract

The ability to control stiffness plays an essential role in soft robotics actuation. One of the most common methods of stiffness control in soft robotics is continuous fiber reinforcement due to the mechanical properties provided by this method, such as higher Young's modulus and inextensibility. Precision and repeatability play a significant role in the robot's performance in continuous fiber reinforcement. Despite the importance of precision and popularity of this continuous fiber reinforcement, most current methods are either manual or limited in patterns. Therefore, this thesis presents a new automatic method to employ conventional Fused Deposition Modeling (FDM) printers to print a loom and employ head changing mechanism to use a fiber extruder to weave the continuous fibers around the loom and create complex 3D geometries required for soft robotics applications. In addition, this work investigated how this method enables us to have more control over the stiffness of the soft material by changing the loom parameters such as diameter and distance and the placement of the pins. Furthermore, inspired by a handcrafting technique, straw weaving, we used the pins to add vertical fibers to the structure to create more actuation possibilities. Various soft actuators were fabricated to present the method's capability in creating complex and 3D structures.

Furthermore, the flexibility and high load capacity of fibers make them a promising material for the fabrication of new types of hinges. Unlike soft hinges, fiber-based hinges provide high axial forces, and can bond more easily to rigid substrates than currently used soft materials. These properties enable the development of hybrid robotics that combine the advantages of both soft and rigid components. To fully utilize the potential of fiber-based joints, we developed a novel fiber embedding technique where the fibers are precisely placed along defined paths and encapsulated with thermoplastic material for bonding. Using this technique, we fabricated a fiber-based joint that outperformed currently available soft joints.

Acknowledgement

To Roham, Ali, Saba, and all the friends that are not here with me. Always remember you guys.

Contents

Chapter 1

Introduction & Literature Review

1.1 Soft Robotics

Conventional rigid robots have been employed in various applications, such as industrial manufacturing, and they efficiently perform the single task they are programmed to do. However, despite the progress made in robotics over the past few decades, adaptability, safe interaction with humans and the environment, and manipulation in undefined structures have remained among the main challenges. As a result, many studies have been conducted to provide solutions to these challenges. However, most of the proposed methods require complex control, sensory, and actuation systems to achieve such tasks [1], and in most cases, they are only suitable for a specific set of tasks [1].

Therefore, scientists have focused on bio-inspired design and how animals interact with the environment to overcome this shortcoming. In nature, even the simplest animals and insects are capable of interacting without requiring complex sensors or controllers due to their physical intelligence. As a result, a new field of robotics has emerged, namely soft robotics, which uses compliant materials instead of rigid links and joints [2]. Thanks to nature-inspired design's softness and low Young's modulus of soft materials, soft robots can safely adapt to the environment and interact better with unstructured environments than conventional robots [1], which makes it suitable for tasks such as safe human interaction or grasping fragile items 1.1.

In addition, unlike conventional robots, where links and joints can be specified, soft robots undergo continuum deformation, which makes links and joints redundant 1.1. Such deformation in the soft robots not only further enables them to interact with the surrounding but also makes them suitable for tasks that are not possible with conventional rigid robots. To benefit the most from these capabilities, various soft robots have been developed for a broad range of applications, such as soft manipulation [3], surgical robotics [4] [5], exoskeletons [6], manipulation in confined spaces [7], and bio-mimetic robots, such as an octopus arm, for complex tasks [8] (1.1).

1.2 Fiber Reinforcement & application in soft robotics

Fiber reinforcement is a technique in the composite industry used to improve the mechanical properties of various materials such as plastics, polymers, metals, and concretes. Due to the high mechanical performance and the lightness of these composites, they have been widely used for various applications from sports materials [13] to industrial applications such as turbine blades [14] and airplane components [15]. The increased stiffness of these composites results from fiber type, fiber density,

Figure 1.1: Soft robotics in general (A) Range of robots category from rigid-link to soft robots [9], (B) soft robots provide a safe interaction with human due to compliant inheritance [10], (C) possibility of grasping fragile object without requiring complex control systems, [11] (D) applications of soft robotics in biomedical exoskeletons and surgical manipulation [12]

and the pattern which defines the mechanical properties [16]. In addition to enhanced mechanical properties, fiber reinforcement has provided a solution to create bonding between two different materials, especially in implant applications, to create strong bonding to human tissues [17], since they can interweave with the tissues and provide durable bonding.

Besides the mentioned advantages, in soft robotics applications, fiber reinforcement plays a more significant role since the fiber material, density, and pattern not only improve the mechanical properties but also can be used to create actuators by controlling the deformation of the soft materials [18] in the inflatable structures.

In fiber-based soft actuators, the fiber's pattern and materials define the motion of actuators. Over the past few years, researchers have investigated various patterns and materials [19, 20] to fabricate fiber-constrained soft actuators. For instance, Suzumori et al. [21,22] designed a new bending actuator by radially reinforcing the soft material. Conolly et al. [18] demonstrated how various radial and axial fiber reinforcement patterns create bending, twisting, expansion, and extension. In addition to simple actuation, many studies have been conducted to create more complex geometries and motions such as heartbeat [23], heart valve [24], and shape-morphing surfaces [25] using fiber. Therefore, changing fiber patterns enables soft roboticists to fabricate the desired motion for their application.

In addition to using fiber patterns to control the deformation of fluid-based actuators, many scientists have embedded functional fibers inside the soft robotics application to create sensors, actuation, signal transmission, and energy harvesting [26]. For instance, by using conductive fiber, various types of soft sensors, such as resistive [26] [27] [28], capacitance [29], and inductive sensors [30], were fabricated. Moreover, active fibers such as shape memory alloys [31] [32] or electroactive polymers [33] [34] were applied to actuate the robot directly. Hence, fiber reinforcement not only improves the mechanical properties of soft materials but also provides a wide range of possibilities in fabricating a variety of soft actuators and sensors.

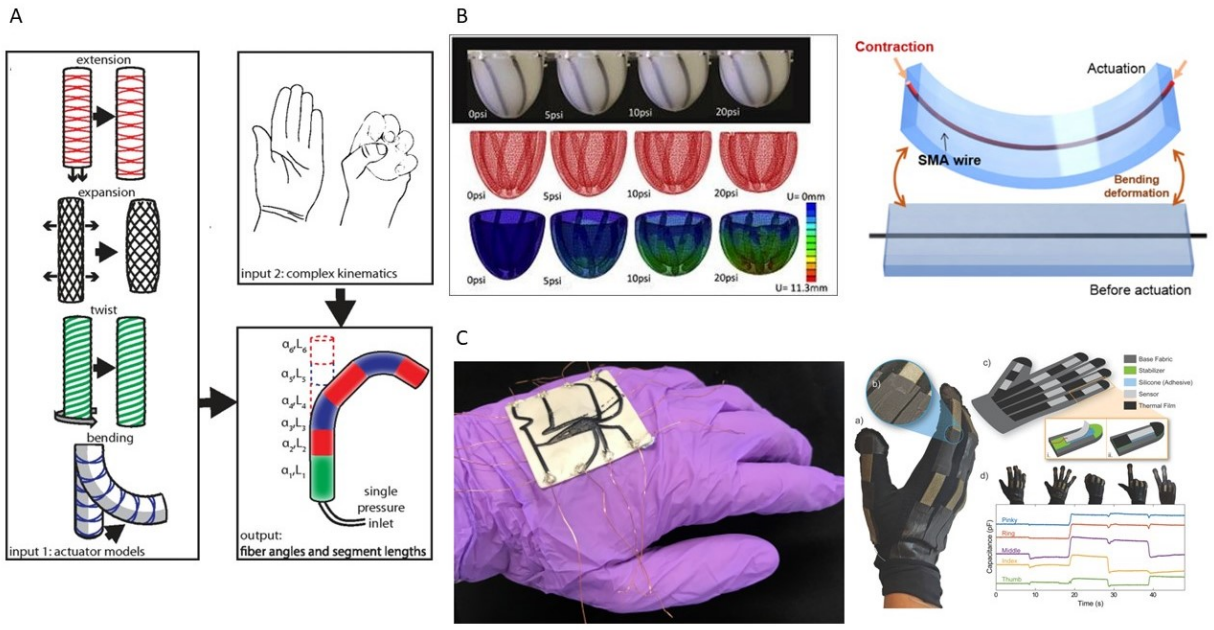

Figure 1.2: application of fiber in soft robotics (A) reinforcing the inflatable soft actuator to achieve various motions [18]. (B) Employing active fiber such as shape memory alloys (SMA) or electroactive polymer as a source of actuation [23, 31] (C) Using flexible conductive fiber and textile as sensory solution [27, 35]

1.2.1 Fiber Embedding Automation

In fabricating actuators using pattern, accuracy and repeatability figure prominently since the slightest misplacement effect the actuator motion and performance [36]. However, the most commonly used fiber embedding technique is either manual by predefined grooves on the actuator [18] [37], which can be cumbersome and lead to inaccuracy, or using an embroidery machine to stitch the fiber [38], which is limited in pattern and possible materials. In order to automatize the fiber embedding process and make the process repeatable and controllable, various researchers proposed already existing methods in the textile industry in soft robotics. For instance, braiding machines were employed to automatize the fabrication of the McKibben actuator [39, 40] and even sensorize it through this process. In addition, Luo et al. [41] designed various pneumatic actuators and integrated sensing using a programmable knitting machine and controlling balloon deformation by changing the pattern. Furthermore, sun et al. [42] fabricated their shape morphing actuator by using a winding machine to create 2D patterns of fibers. However, unlike knitting and braiding, using a weaving machine directly in soft robotics applications is more complex due to the complexity of weaving patterns and machines. Thus, there have been some works to replicate the weaving process since weaving properties enable high force in soft robots [43]. For example, inspired by an artist [44], Stalin et al. [36] proposed a method to use a predefined loom to weave a 2D structure to increase the material stiffness. This technique was later used to fabricate sensory systems using conductive textile [28], and inductive coil [30] for wearable applications.

Although these fabrication techniques are significant steps toward automating fiber embedding, these methods' current patterns are limited. The pattern limits knitting machines used so far and is unsuitable for creating inextensible textiles due to the extensibility of knitted patterns. Moreover, the braiding machine is only suitable for braiding over a cylinder or limited geometries. The work done in the weaving process only demonstrated deposition in 2D and did not discuss axial fibers, which are crucial in many soft actuators.

Furthermore, to include similar properties as fiber and not be limited by the patterns, some research has been carried out to have multi-material printing. In this method, mainly using Direct Ink Writing, a high-stiffness material is printed together with the soft material to emulate the fiber performance. Schaffner et al. [45], and Coulter et al. [24] 3D printed complex structures using this technique. Despite the application of this method and the possibility to create very complex patterns, conventional continuous fiber reinforcement improves the mechanical properties better than stiffer printed material since they provide more inextensibility and flexibility than the stiffer material. Moreover, the shore hardness and the possible materials for printing more rigid material are limited due to bonding problems and, in some cases printing limitations, and having similar functionality, such as active actuation, is yet to be done with these materials. Finally, there have been numerous studies in industrial systems on embedding the fibers inside the 3D printing structures and co-extruding with the material matrix. However, the materials used in these techniques have high shore hardness, which is unsuitable for most soft robotics applications.

1.3 Soft Robot's Limitation & Hybrid Robots

Over recent years, there has been considerable progress in soft robotics, either in developing new materials, creating new designs, and new control methods for more repeatability of these robots. However, despite the progress, soft robots lack the precision and load capacity that conventional rigid robots provide due to the low stiffness and large deformation of soft materials. In some robotics applications, having high load capacitance and precision is as essential as softness and adaptation. For instance, Bartlett et al. [46] proposed a new bio-inspired combustion robotic design in which they 3D printed a graded material from soft to rigid to benefit from soft exterior and rigid interior.

Moreover, these hybrid characteristics mimic the biology of animals and humans, which benefit from both rigidity and softness. This is accomplished by having inner skeletal structures for rigidity and muscle-based exteriors for softness. For example, in the human body, bones provide rigidity for load-bearing, movement, and protection, while muscles offer a soft interface for interaction with the environment and adaptability. Therefore, hybridity is crucial in creating robotic systems that emulate biological systems.

As such, various studies have been conducted on new designs of hybrid robots. For instance, complaint mechanisms have been intensely investigated as a possible solution for high range of motion and precision simultaneously [47] [48]. However, despite the promising aspect of these designs, the softness and flexibility provided by compliant mechanisms are not comparable with soft materials. Furthermore, these designs require complex computational optimization and a cumbersome designing process. Another approach to hybrid systems is using conventional soft materials such as rubber and rigid materials. However, so far, the bonding between soft and rigid materials has remained a main challenge since the bonding is mostly done by glue which is not repeatable and not robust for many applications. Moreover, to overcome the bonding limitation, Rossing et al. [49] have proposed an interlocking printing in which they printed a thermoplastic grid and used the grid as an interlocking mechanism between the rigid thermoplastic, here PLA to silicone rubber. Despite the intriguing concept in this work, the connection lacks the required flexibility for hybrid robotics.

Similar to other soft robotics solutions, nature can inspire us to solve this shortcoming in the field. In human biology, connective tissues bond the rigid structure of the bones to the soft muscle tissues [50]. The microstructures of the connective tissues are a series of small fibers interwoven into each other and create strong and, meanwhile, complaint structures [51]. Therefore, such properties inspired us to replicate such behavior by employing the fiber embedding method and opening a new possibility of creating hybrid structures.

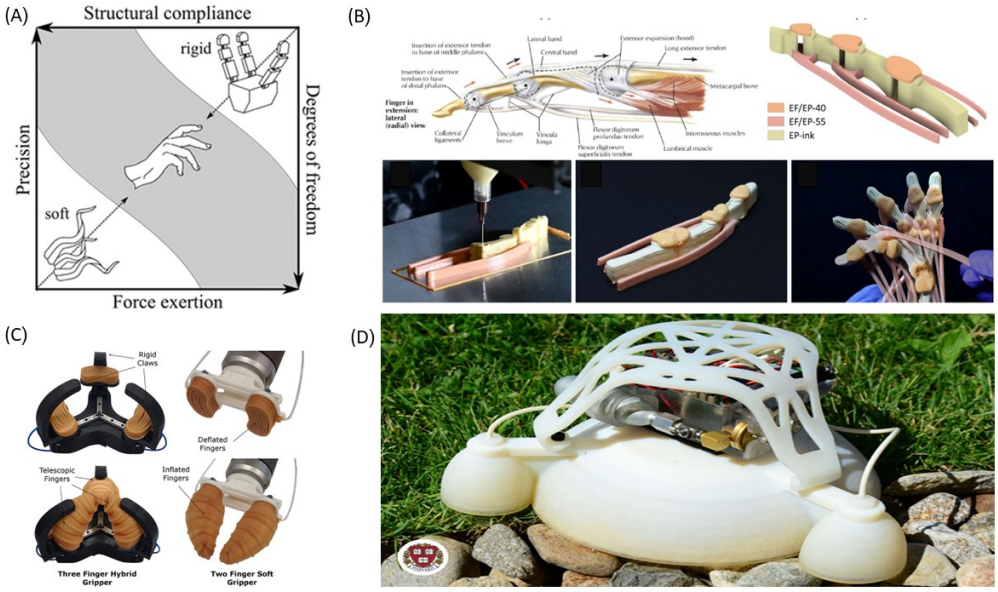

Figure 1.3: Recent Developments in hybrid robotics, (A) The four properties of soft and rigid robots and how they change in this spectrum. [52] (B) a 3D printed hand using soft materials with different shore hardness to mimic hybrid behavior. [53] (C) A hybrid gripper for both precise and safe manipulation. [54] (D) The combustion hybrid robot that consists of rigid tops and soft bottoms. [46]

1.4 Research Goal and Outline of Report

In sections 1.2.1 and 1.3, two of the challenging problems in soft robotics fabrication have been presented. In this thesis, we aim to propose a new automated method that not only enables fabricating complex 3D geometries for various soft robotics applications but also, due to inherent flexibility and high load capacitance, provides a possible bridge between the soft and rigid robots.

Therefore, inspired by [36, 44], we first present a novel technique to automatize the fabrication of complex 3D continuous fiber structures. In this method, we used the Fused Deposition Modeling (FDM) printer to build a base loom for the structure and weave the desired pattern around the loom using a changeable head. Combining loom printing and fiber weaving solves current automatic methods' limitations and enables us to fabricate more complex and repeatable 3D structures. Moreover, printing the loom allows us to achieve desired mechanical properties of soft materials by changing the loom geometry and dimension and, subsequently, fiber pattern easily. Finally, having a printed loom gives the possibility to later add the axial fibers to the structure for various actuator designs.

In the next step, we used path printing with the FDM printer to employ the high load capacitance and flexibility of fibers to create hybrid robots. First, we investigate the bonding between PLA and fiber and how the fibers can be directly used to create fiber-reinforced joints that are quite compliant compared to the current soft joints [55, 56], tolerate higher axial forces compared to these joints, and provide the inextensibility suitable for many applications. Finally, to emulate the connective tissue functionality, we investigate fibers as bonding points between 3D printed material and soft rubber.

Chapter 2

Material and Methods

2.1 Fiber Reinforcements Classification

Section 1.2 provides an explanation of how fiber reinforcement is utilized to enhance the mechanical properties of materials. Depending on the specific requirements of the fiber-reinforced structure, the size, continuity, pattern, and type of fiber used can vary. There are three main categories into which fibers can be classified based on their size and continuity: particulate reinforcement, short fiber reinforcement, and continuous fiber reinforcement. Particulate reinforcement involves the insertion of small reinforcement particles into the material matrix [57] [58]. This type of reinforcement is typically employed when minor changes in stiffness are necessary and is favored for its ease of mixing the particles into the matrix [59].

Short fiber reinforcement involves the placement of discontinuous fibers within the material matrix [60]. This type of fiber reinforcement is commonly used in the aerospace and automotive industries and provides significantly higher strength than particulate reinforcement [61, 62]. Continuous fiber reinforcement involves embedding fibers without any interruption within the matrix [57] (refer to Fig2.1). This method of fiber reinforcement provides the greatest strength compared to the other techniques. Several studies have investigated the integration of short and particulate fibers in soft robotics systems, as each of these reinforcement approaches enhances mechanical properties differently. Nonetheless, previous research has demonstrated that continuous fibers are the most effective reinforcement solution for inflatable soft actuators [22]. Particle and short fiber reinforcement cannot provide the desired inextensibility for most inflatable soft actuators. Therefore, our focus here is on fabricating 3D continuous fiber structures.

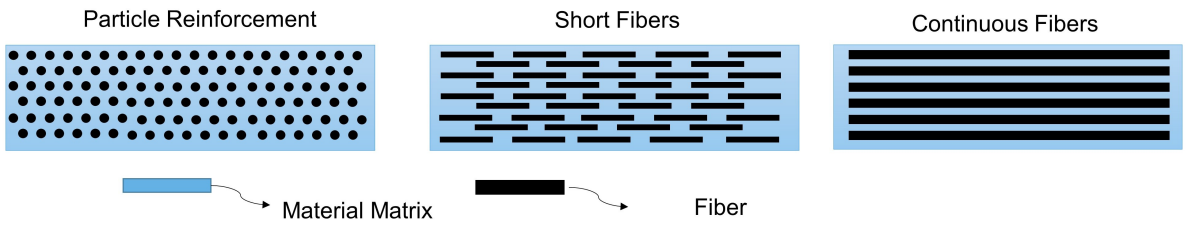

Figure 2.1: Different categories of fiber reinforcements based on the fiber size in the polymer.

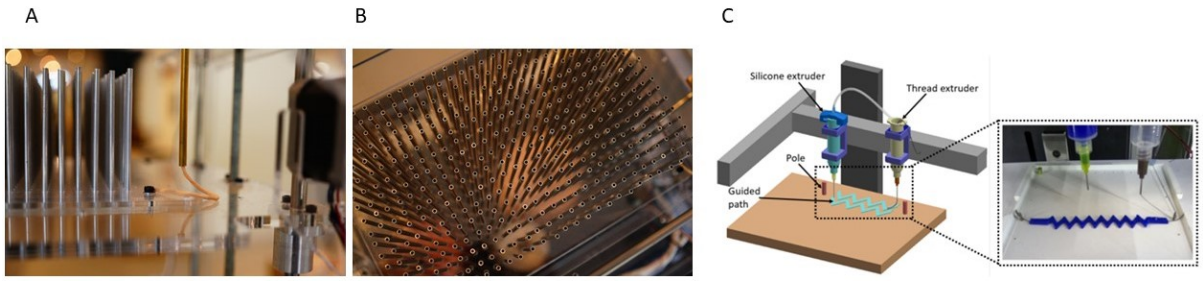

Figure 2.2: The two previously developed techniques for automating weaving embedding. (A)(B) Using a base of rigid pins as a loom and tie one end of the fiber on one side of the bed and pull the fiber through the nozzle with the Capstan effect. The fiber is constrained in this method by the pins. (C) Make a path and define the fiber placement by the path, and deposit material on the fiber to ensure their embedding.

2.2 Automated Continuous Fiber Embedding

Continuous fiber structures can be categorized into braiding, knitting, and weaving based on the fiber pattern. Woven textiles are particularly advantageous for their inextensibility and ability to produce high-force inflatable actuators. To create woven textiles, commercial machines hold the warp fibers stationary and under tension while the weft fibers are drawn through and placed over and under the warp. Although commercial weaving machines are speedy and reliable, utilizing them to automate fiber reinforcement embedding and make it programmable poses difficulties due to the machine's size, complexity, and limitations in 2D patterns. Another challenge in fiber deposition is the flexibility of fibers, which can only be pulled and not pushed, unlike 3D printing filaments. Additionally, fibers cannot be plotted without constraints as they tend to follow the machine head.

In order to address the limitations of weaving machines and resolve issues related to fiber placement, two potential solutions are available. The first involves using pins to guide and pull fibers through the nozzle, facilitating their placement. The second method entails defining a specific path for the fibers to follow, allowing them to be passed through and held securely in place. (Fig2.2)

2.2.1 Loom Printing

An artist proposed a new technique to make the deposition and embedding of continuous fibers programmable [44] in order to overcome the limitations of weaving machines. The artist first created a predefined loom out of metallic pins at the desired position. Then, one end of the fiber was tied to a pin to pull the fiber with the Capstan effect, a gantry system was used to pass the fiber around the pins, and complex geometries were created. With this method, 3D woven structures could be fabricated without requiring further steps such as stitching and sewing.

However, this method has limitations due to the pre-made metal pins, which limit the diameter, height, and position, as well as the narrow patterns in 3D. To increase flexibility, we propose a method in which the pins are printed using an FDM printer, and the fibers are woven around the printed pins (Fig2.3). Printing the pins enables us to change the pins' diameter, height, position, and distance, making the process less time-consuming and challenging. In addition, this technique can print non-vertical pins, significantly increasing the possible patterns. This additional flexibility is beneficial, especially in soft robotics applications, where the fibers determine the elastic properties of the soft material, which then determines the actuator's behavior. Automating the fiber deposition

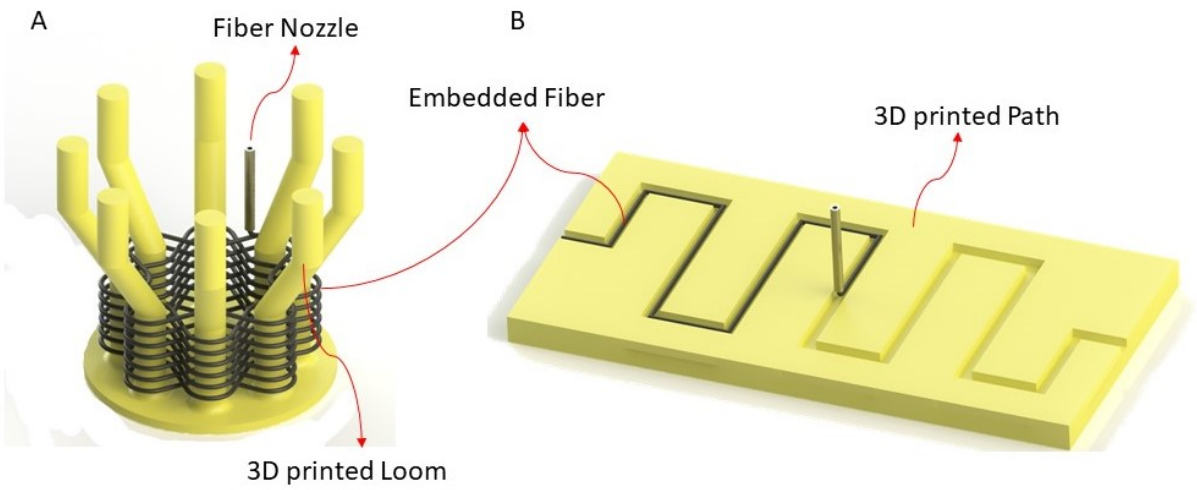

Figure 2.3: The two proposed methods to combine FDM 3D printing with fiber embedding. (A) Printing a loom and weaving around. The printing of the loom provides higher flexibility in creating non-planar structures. (B) Printing the path and embedding the fiber inside the path.

and the flexibility that 3D printed loom provides increases the possibility of changing and tuning the soft material's elastic properties depending on the application. Furthermore, using the 3D printer, the air path required for inflation of soft pneumatic actuators can be integrated inside the pin printing, working towards more automated fabrication.

In addition to the extensive range of patterns and applications that weaving around the pins can create, vertical fibers play an essential role in the actuator performance in some fiber-reinforced soft actuators. For example, in the bending actuator, the axial fiber reinforcement improves the bending performance by reducing the axial deformation, while the vertical fiber increases the possible actuation, such as twisting [22]. Inspired by straw weaving, a handcraft technique, we removed the pins from the woven structure, creating a hole inside the structure that allowed us to insert the vertical fiber later. In addition, removing the pins in a 3D-printed loom can be more manageable since the pins can be printed with water-soluble materials that can be washed away.

2.2.2 Path Printing

One approach to accurately position fibers involves moving them along a 3D-printed predetermined path (Fig2.3). In this method, the wall of the paths defines the position of the fiber. Stalin et al. [28] first utilized this technique by printing a guide wall with a soft material matrix through direct inject writing. However, this method only facilitated embedding fibers in a single layer and producing simple patterns. Similar to the loom printing method, the FDM printer enables the printing of more intricate paths in 3D geometries and printing in Z-axis.

Furthermore, we can adopt the same technique as loom printing to embed fibers within the paths and subsequently deposit material over the fibers using the FDM machine to prevent movement within the slots. This technique is particularly advantageous for hybrid designs and bonding to rigid materials since the covering material can be a rigid thermoplastic extruded or deposited over the fiber path, and the fibers can serve as bonding media while providing softness and softness strength to the structure. In this thesis, we first employ this method to benefit from the flexibility of the fiber in the fabrication of high-load capacitance and soft hinges. In the second stage, the fibers are used as bonding points between the 3D-printed material and the soft rubber.

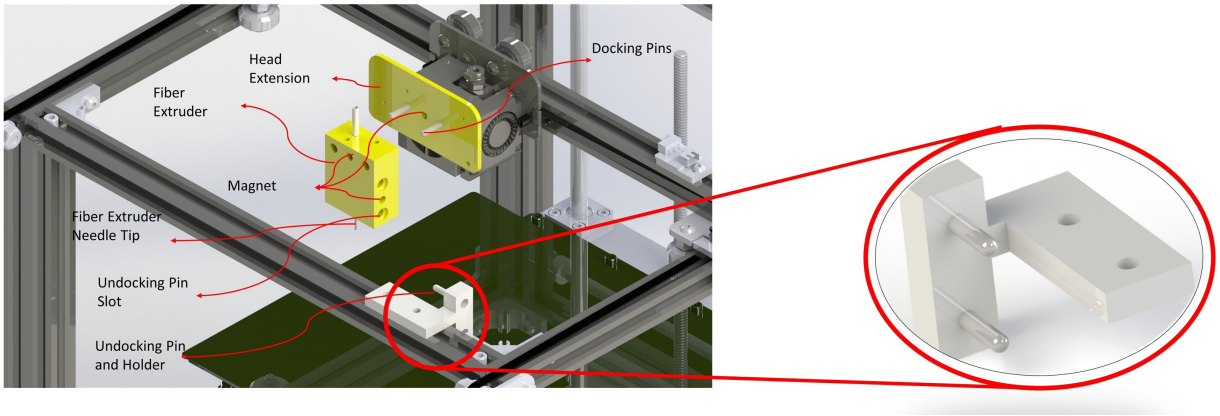

Figure 2.4: The modification and the head exchange mechanism designed for the Creality ender 5 printers. Unlike commercial systems, this head-changing mechanism does not require an additional motor and enables a more complex weaving pattern.

2.3 The Machine and Process

2.3.1 Machine Design

Regarding machine design, our approach involves printing either a loom of pins or a path and then weaving the fiber, as explained in the previous section. Therefore, we require the utilization of a multi-material printing method. Multi-material printing techniques can be categorized into six main methods, as detailed in [63]. Among these methods, the tool-changing mechanism is best suited for printing and weaving since continuous fiber can interrupt the loom printing process when using other multi-material techniques.

Moreover, the current tool-changing mechanisms available in the market necessitate the installation of extra motors and electronic boards. Therefore, to integrate the fiber weaving process into a single nozzle FDM printer commercially without incurring additional electronic and control complexities, we modified the printer head and added a new fiber extrusion tool to the machine, as illustrated in Fig2.4.

In this design, we employed magnets and two degrees of freedom to dock and undock the fiber extruder. A station with two pins and a magnet is mounted on the machine frame, and similar designs are present on the machine head (Fig2.4). The pins on the station and machine head are perpendicular to each other, so by initially moving in the Y direction and then in the X direction, the fiber extruder docks to the machine head, and by moving oppositely, it undocks into the frame station. These modifications are tailored for Creality Ender5 and can be adapted for other printers as well. Concerning the fiber extrusion, the fiber extrusion tool comprises a needle tip to guide the fiber through the loom, a tensioner to regulate the fiber's tension, and pin holes for the docking mechanism to be mounted either on the head or the frame station. Furthermore, in addition to the tool changing and fiber extrusion tool, we appended a pin to the printer's frame to fasten one end of the fiber at this pin and pull the fiber through the weaving process.

2.3.2 Weaving Process

Weaving Process with Printing Loom

As for the process, in the 3D weaving shown in Fig2.5, the loom prints are divided into several parts based on their printing height. After printing each of these parts, the machine changes the head and weaves the desired pattern around the loom, and then the machine changes to FDM printing and continues loom printing. This iteration is continued until the print is completed. This procedure enables us to make the distance between the pins smaller and has taller pins, thus creating finer and longer woven textile. Furthermore, with this technique, the needle tip can be shorter than the method developed by the artist. As a result, the diameter of the needle can be smaller without fiber tension deflecting the needle tip and causing errors in the print. In addition to finer print, pausing and weaving at certain heights enables the creation of more complex geometries since in some patterns, such as twisting, the pins are not vertical, and without pause, weaving with a gantry system and needle tip is not possible.

After the print is completed, a soft material is deposited around the woven loom to the fiber inside the soft material that we desire to reinforce and keep the fibers in their place, even after removing the pins. The mold for the soft material can either be directly printed during the weaving process or later be added to the structure. After the soft material is cured and the soft fiber reinforced structure is fabricated, we remove the pins either by taking them out or solving them in water, depending on the 3D printed material.

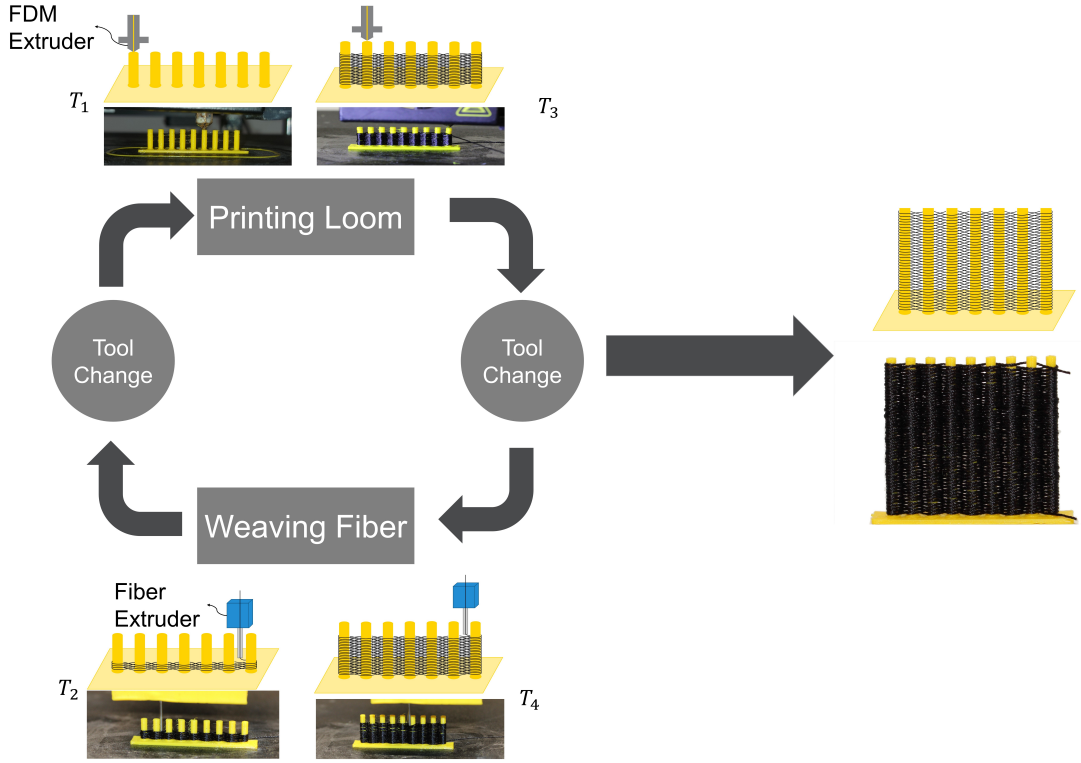

Figure 2.5: The iteration demonstration of the loom printing and weaving process. In this process, first (T_1), the FDM printer prints the loom, then the machine changes its head (T_2) and uses the fiber extruder to place the fiber around the pins. This iteration continues until the desired structure is fabricated.

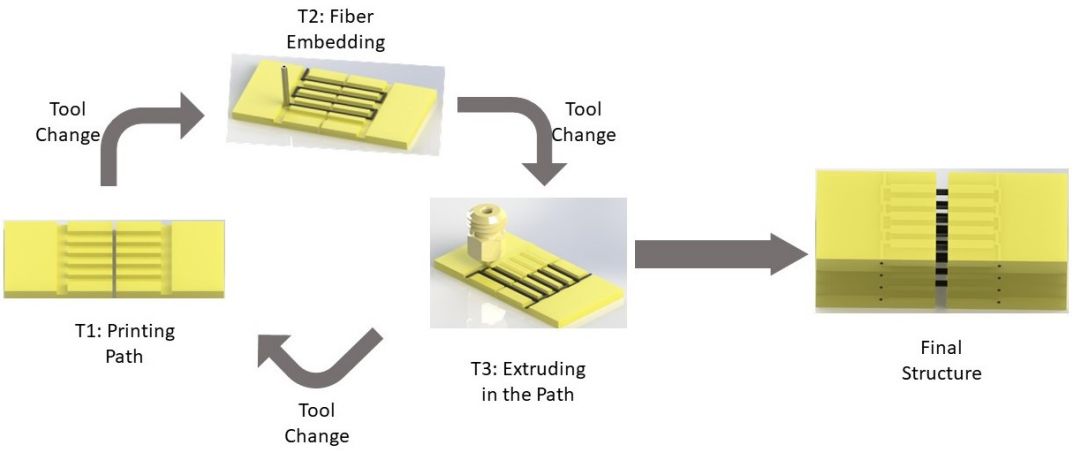

Figure 2.6: The process of printing path and embedding the fiber with the 3D printer (T_1), the FDM printer prints the base structure with the path. (T_2) The machine changes the head, and the fiber needle tip moves through the path to place the fibers. (T_3) The machine changes the head and extrudes on top of the fibers to fill the cavity and ensure the fibers embedding. This iteration is continued until the whole structure is fabricated.

Weaving Process with Path Printing

In this method, similar to loom printing, we first print the desired fiber paths, then the machine changes the head and moves the fiber through the paths. After each iteration, there are two possibilities, either fix the fibers instantly by extruding the thermoplastic material after the weaving step is finished or finish the whole process and deposit the material similar to the previous method. In the process of printing the 3D printed hybrid structure as shown in Fig2.6, first, the base of each link with the fiber paths is printed. Then, the fiber is embedded inside these paths, and the thermoplastic PLA is instantly deposited to avoid fiber slippage. After finishing the extrusion, the FDM printer continues printing the rest of the joints until it reaches the next place where the fiber must be embedded.

2.3.3 G code Generation Process

In order to communicate with the 3D printer, G-code is required to be generated. First, based on the desired fiber pattern, a loom or path is designed using CAD design software (such as SolidWorks). Later, the CAD file is exported into the slicer to generate the Gcode. To generate the Gcode for the fiber extrusion, however, the normal slicers available are unsuitable since most slicers do not provide the ability to control the tool path, which is vital in fiber deposition. Thus, the fiber extrusion Gcode is generated using a Grasshopper, an extension of Rhinoceros 3D software. This software provides a platform in which the desired fiber path can be drawn, and the Gcode for such paths can be generated from this software. In the final stage, python is employed to merge and add the required pause to the generated code from both Grasshopper and Cura slicer, and the finalized code is given to the machine (Fig2.7)

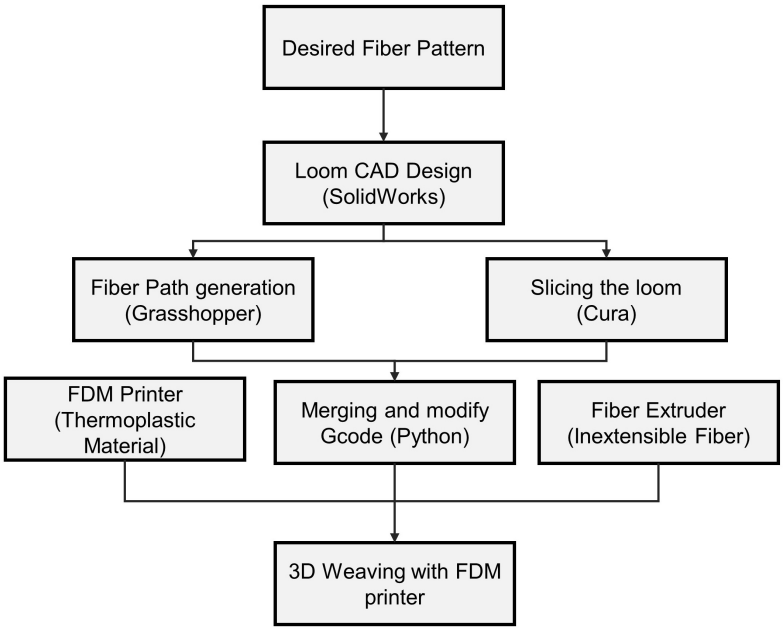

Figure 2.7: Workflow of the weaving process, first, a loom is designed depending on the desired fiber pattern. Thereafter, the loom is sliced in Cura, and the fiber path is generated. Later, the thermoplastic material, the fiber, and Gcode for both loom printing and fiber weaving is added to the machine to start the process.

2.3.4 Materials

In this study, we employed four different types of materials with distinct functionalities to print the loom. The four filaments used were Polylactic Acid (PLA), Polyethylene Terephthalate (PET), Polyvinyl Alcohol (PVA), and Lay-fomm 60. Each of these materials offers unique properties during the weaving process. PLA is a widely used material that can be effortlessly printed. PET is utilized for its high mechanical strength and ease of printing, while PVA is water-soluble and allows for easy removal of pins after embedding fibers. Lastly, Lay-fomm 60 is a PVA-rubber hybrid material that is rigid during printing but becomes flexible after washing in water, due to the removal of PVA particles.

However, in the fabrication of the hybrid hand gripper, only PLA was utilized as the substrate printing material. Furthermore, to compare the performance of the proposed design with existing designs, Ninjaflex TPU was printed and utilized as a benchmark.

For the fiber, we utilized 100 % Bonded nylon (SomaBond 40) with a diameter of 0.2mm. This fiber was selected due to its non-extensibility and high mechanical strength, which surpasses that of most commercially available fibers. Lastly, as the rubber material, we chose Ecoflex 00-10 (Smooth ON), which is a commonly used material in the production of soft robots.

2.3.5 Theory

As previously mentioned, fiber reinforcements in inflatable soft actuators are important since they control the stiffness and extensibility of the soft material. One of the primary sources of the stiffness change is the fiber pattern in the matrix of soft material. Since in our 3D weaving technique, the pins can be printed in different sizes, different locations, and in non-planar directions, this method

renders us capable of modifying the stiffness and extensibility depending on the application by just changing the pattern of fiber in the matrix. Although using our method, various fiber-based patterns can be fabricated, all the fiber around the pins can be divided into two main patterns as shown in Fig2.8. In pattern 1, since the pins are in one line, the fibers can be passed on both sides of the pins. On the hand, in pattern 2, the fibers can only pass on one side of the pin to create the anchoring point required for pulling the fiber.

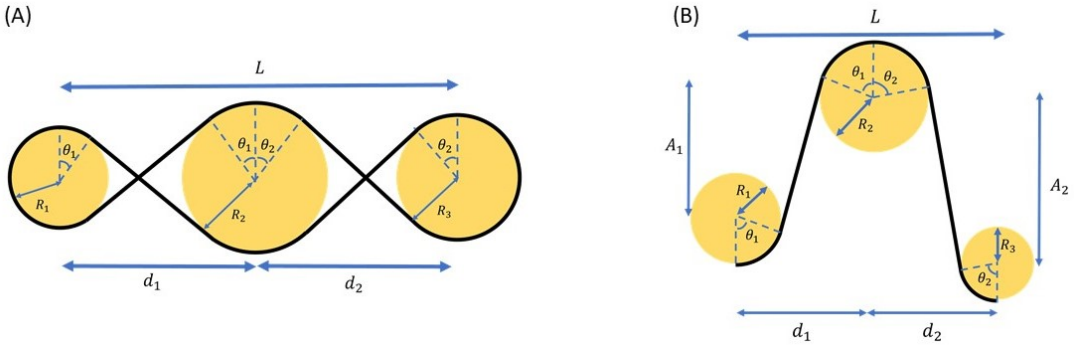

Figure 2.8: The possible extensible fiber pattern using the proposed method that enables material stiffness control, (A) a double side pattern in which, like conventional weaving, the fiber passes both sides of the pins. (B) the serpentine pattern in which the fiber pass only one side of each pin in the loom.

For the first pattern, the extensibility of the manufactured woven structure can be calculated by deducting the distance between the center of the first and last pin from the woven fiber length.

$$\begin{aligned} L_f &= (R_1\theta_1 + R_2\theta_1 + d_1 cos(\theta_1)) \\ &+(R_2\theta_2 + R_3\theta_3 + d_2 cos(\theta_2)) \\ where\ \theta_i &= \frac{\pi}{2} - cos^{-1}(\frac{R_i + R_{i+1}}{d_i}) \end{aligned} \tag{2.1}$$

Where, as shown in Fig2.8-(A), R_1,R_2, and R_3 are the radius of the respective pin, d_1 and d_2 are the distance between two consecutive pins, and L_f is the woven fiber length. This equation shows that the distance and diameter of the pins decide the extensibility in the first pattern. Assuming that the pins are the same diameters, the distances are equal, and repeated n times, we can simplify Eq2.1 as shown in Eq2.2.

$$\begin{aligned} L_f &= n(2R\theta + dcos\theta) \Longrightarrow \\ \Longrightarrow Extensibility\% &= \frac{L_f}{L} = \frac{2R\theta + dcos\theta}{d} \end{aligned} \tag{2.2}$$

In addition, for the second pattern, the extensibility is similar to the first pattern with the addition of amplitude (A_1 and A_2) which, as shown in Fig2.8 is the out-of-line distance between the center of two consecutive pins. Therefore, the extensibility is as follows:

$$\begin{aligned} L_f &= (R_1\theta_1 + R_2\theta_1 + \sqrt{A_1^2 + d_1^2}sin(\alpha_1)) \\ &+(R_2\theta_2 + R_3\theta_3 + \sqrt{A_2^2 + d_2^2}sin(\alpha_2)) \\ where\ \theta_i &= \frac{\pi}{2} - cos^{-1}(\frac{R_i + R_{i+1}}{d_i}) + tan^{-1}(\frac{A_i}{d_i})\ \& \\ \alpha_i &= cos^{-1}(\frac{R_i + R_{i+1}}{d_i}) \end{aligned} \tag{2.3}$$

Similar to Eq2.2, equation Eq2.3 can be simplified if the amplitude, the distance between the pins, and the pins' diameters are the same across the loom.

$$\begin{aligned} L_f &= n(2R\theta + \sqrt{A^2 + d^2}sin\alpha) \Longrightarrow \\ \Longrightarrow Extensibility\% &= \frac{L_f}{L} = \frac{2R\theta + \sqrt{A^2 + d^2}sin\alpha}{d} \end{aligned} \tag{2.4}$$

In order to find Young's modulus of the fiber-reinforced material, the rule of the mixture as shown in Eq2.5 is used. In this equation, V_f is the fiber volume, V_m is the volume of the soft material, E_f is Young's modulus of the fiber,E_m is Young's modulus of the soft matrix, and E_c is Young's modulus of the composite.

$$E_c = \frac{V_f}{V_m + V_f}E_f + (1 - \frac{V_f}{V_m + V_f})E_m \tag{2.5}$$

On the other hand, the important calculation for fiber embedding with path printing is the extrusion rate required to fill the fiber gap with the thermoplastic material to ensure the fiber bonding to the substrate. The extrusion rate over the gap can be calculated as follows:

$$E = \frac{h * L * W - \frac{\pi * D^2}{4}}{\pi * \frac{d^2}{4}} \tag{2.6}$$

Where h is the path's height, L is the length between two consecutive points in Gcode, W is the width of the sloth, D is the diameter of the fiber, and d is the diameter of the thermoplastic filaments.

2.3.6 Experimental Setup & Protocol

Fiber Reinforcement of Soft Materials Experiments

As explained, the fiber reinforcement pattern determines the soft materials' stiffness. In addition, as shown in Fig2.8, all the patterns created using our method can be divided into two base patterns. Thus, we performed two experiments to characterize how each fiber reinforcement pattern influences the stiffness of soft material in the direction of the fiber reinforcement. Moreover, using the proposed technique, a vertical fiber can be placed in the cavity after removing the pins to reinforce the structure in the other direction. Therefore, another experiment was performed to investigate the effect of vertical fiber in reinforcing the soft material. To perform all the tests, A universal tensile test machine (Instron 3343, Instron, USA) with the shown setup (Fig 2.9) was used.

In the first experiment, we characterized the first pattern with a setup shown in Fig2.9-(A). In Eq2.2, the structure's extensibility depends on the pins' diameter and the number of pins over a

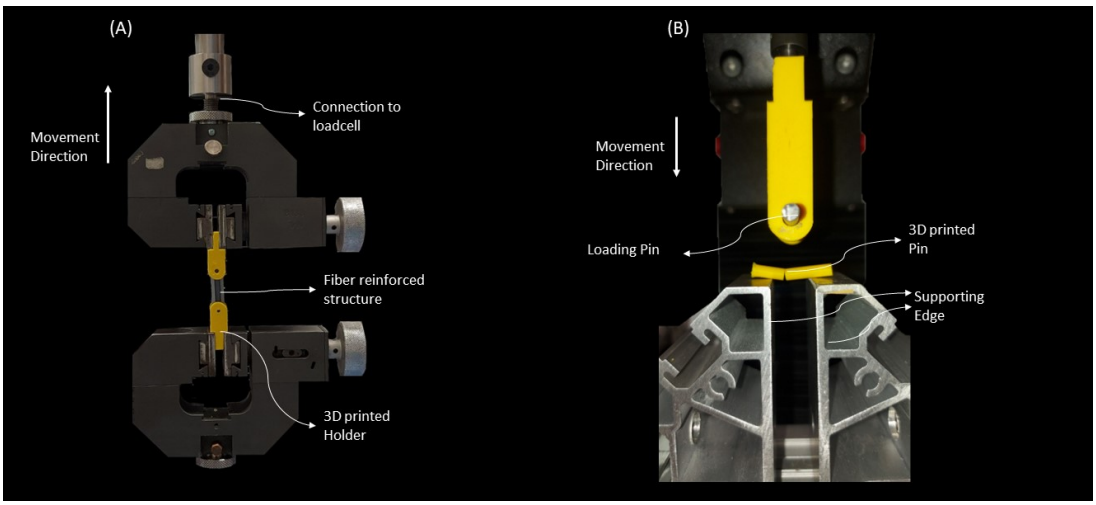

Figure 2.9: The experimental setup used with Instron tensile tester. (A) the setup for two side extension test, (B) the pins bending experiment setup.

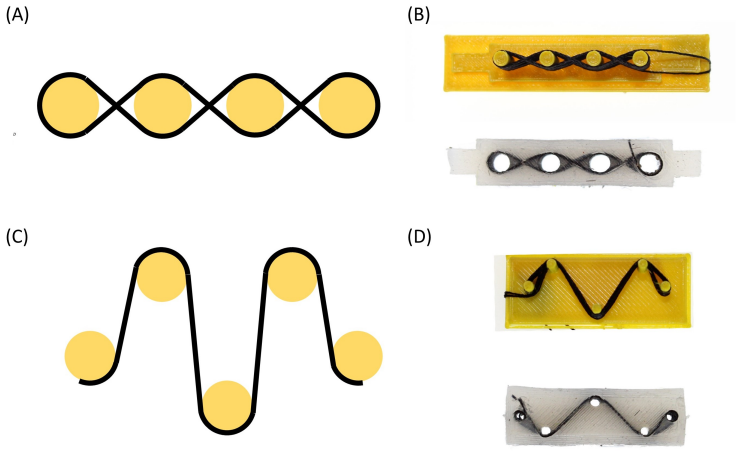

Figure 2.10: The test sample used for extensibility and stiffness experiment, (A) the weaving pattern for two side and vertical fiber extensibility. In this test, we changed the number and diameter of the pins. (B) the actual woven fiber and embedded in a silicone rubber sample. (C) The one side serpentine pattern. In this test, we changed the number of pins, therefore, the distance between the pins. (D) The actual one-side woven fiber and embedded in a silicone rubber sample

certain distance (the distance between the pins). Hence, to exhibit how each parameter affects the extensibility, we perform a tensile test on the samples (Fig2.10) with various diameters (2-3-4mm) and various numbers of pins (2-4-6) under Instron with a strain rate of 100%/min. First, with 4 Pins, we changed the pins' diameter (2-3-4mm). Then, with a diameter of 2mm, we changed the number of pins (2-4-6). In all of these prototypes, the distance between the center of the first and last pin was 28mm. Furthermore, due to the load cell limitation on the Instron, we limited the maximum tensile load to 200N.

A similar experiment to the first pattern was performed for the second weaving pattern. A sample shown in Fig2.10 was fabricated to test the stretchability of the soft material after the fiber reinforcement using the second pattern. In this case, over a certain distance between the first and last pin (30mm), the number of pins was changed (3-5-7-9 pins) to investigate how changing the angle of the serpentine shape would change the stiffness.

As mentioned, our method enables vertical fibers in the structure. Therefore, we performed a test to study how vertical fiber reinforcement influences the soft materials' stiffness. Therefore, samples with a similar pattern to Fig2.10-(A), but with a height of 40mm, were fabricated. In these samples, over a certain distance of 20mm, we changed the number of pins from two to five pins. At first, we experimented without placing the vertical fiber and stretched it to 50% of the original length of the sample. Then, vertical fiber was inserted and extended to evaluate the impact of adding vertical fiber and increasing the number of vertical fibers in the stiffness. After adding vertical fiber, the test was done until only 5% of the total length since the vertical fiber prevents further extension.

Finally, we used four different materials to print the pins. During the printing process, the capstan effect of the fiber tension applies a shear force to the pins, which may lead to deflection or breaking of the pins. Therefore, high bending stiffness and breaking point under shear load are essential for pins. Therefore, to compare how these materials behave under shear force, we performed a 3-point bending test with a setup shown in Fig2.9. The pins in this test had a diameter of 4mm and a length of 30mm. The distance between the two stands of the bending setup was 20mm.

Hybrid Structure Experiments

As discussed in 1.3, hybrid joints offer significant advantages such as high axial load capacity and low bending forces. In light of this, we conducted experiments to compare the axial force and bending stiffness of fiber-based joints with newly developed soft joints.

In the first experiment, we aimed to determine the optimal extrusion rate for encapsulating the fiber inside the path to achieve the highest axial load. We used the geometry shown in Fig2.11-A and tested different extrusion rates (ranging from 20 % to 140%) at a strain rate of 100%/min. In the second experiment, we investigated the effect of increasing the number of slots in the path on the axial load capacity. We repeated the previous experiment, this time varying the slot number (2-3-4-5), using the similar setup illustrated in Fig2.3.6-A.

To compare the performance of the fiber-based joint with TPU-based hinges, we printed a configuration with the same dimensions as [55] using Ninjaflex and a 9-slot woven hinge with an extrusion rate of 120%. We subjected both hinges to a strain rate of 100%/min until they broke. Additionally, we performed a cyclic test on the hinge, subjecting it to 1000 cycles with a load limit of 100N to investigate the repeatability of the test. In addition, we also conducted a 3D point bending test on both the woven and Ninjaflex joints to compare their bending stiffness. Due to the angle limitation of the joints, the test was performed only until 5mm compression.

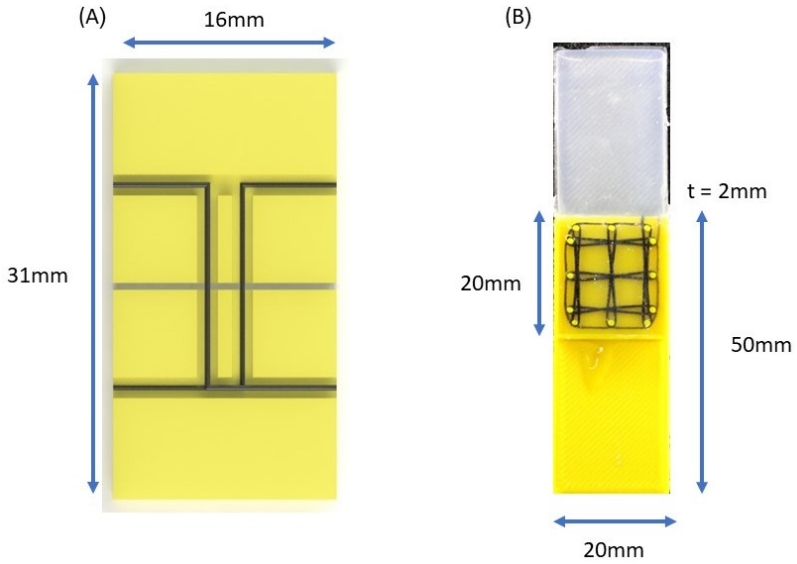

Figure 2.11: The samples for the path printing tests, (A) the sample schematic used to find the optimized parameters for bonding between PLA and fiber. (B) the lap shear test sample was used to measure the bonding between silicone rubber and PLA with fiber interface.

Lastly, we used the fiber structure as a bonding point between soft rubber and thermoplastic filament. Therefore, we performed a standard lap shear test on fiber-based structure as shown in Fig2.11-B, and compared it to the same structure connected with glue. Due to the 3D printing volume limitation, the dimensions were scaled down to the dimension in Fig2.11-B. The speed for this test was 10mm/sec. Moreover, we printed with 3, 4, 5, and 6 pins to investigate the effect of fiber density. Regarding the material, similar materials as the previous experiment were used. For the glue to stick the silicone rubber to PLA, silicone glue with a shore hardness of 25A was used.

2.3.7 Prototypes

Several soft actuators and fiber structures were fabricated to demonstrate the application of the proposed method in soft robotics. First, by placing the pins around a cylinder pattern (Fig2.12-(A) and weaving the fiber radially around the structure, an extensible actuator was fabricated. Later, with the same pattern of pins and radial fibers, by just adding vertical fibers through holes on one side after removing the pins (Fig2.12)-(B), a bending actuator was created. Moreover, the cylinder would behave as a stiff beam by passing vertical fibers through all the pins' placement. Finally, using the same fiber pattern, a twisting actuator can be fabricated by only twisting the pins as shown in Fig2.12-(C) and passing vertical fibers. Fabricating the twisting actuator exemplifies how our 3D weaving method is capable of creating patterns that are not possible with other techniques.

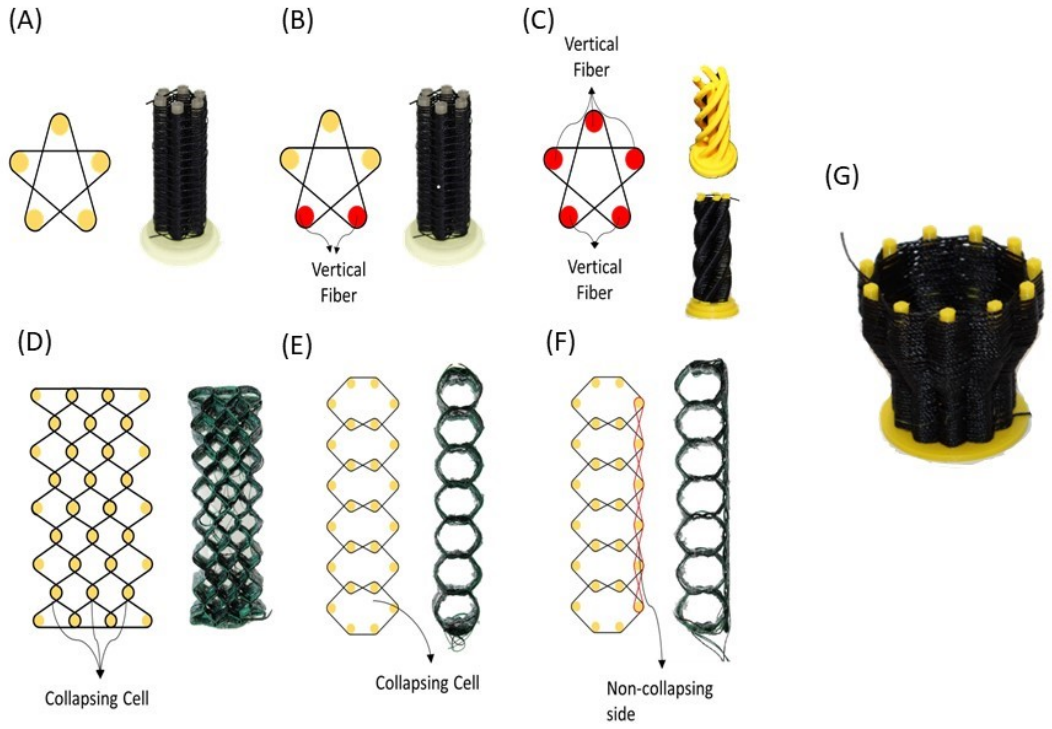

Figure 2.12: Different inflatable actuators made using the proposed method. (A) the pattern schematic and the woven structure for the extension actuator. In this actuator, the cylinder is only radially reinforced. (B) Adding two vertical fibers at one side of the previous structure provides bending actuation. (C) Using a 3D printer and changing the head mechanism, we can twist the pins and create twisting actuation. Example of possible patterns and vacuum actuators fabricated using our method. (D) a contraction actuator with diamond shape cells. (E) a contraction actuator with honeycomb geometry. (F) a bending actuator by adding a line of non-collapsing side to the previous actuator. (G) a 3D woven vase as an example of non-planar 3D printing.

In addition, three different vacuum actuators were fabricated to show more broad patterns that can be created using this technique, as shown in Fig2.12. The aspect ratio between the contracting and non-contracting sides in two contraction actuators helps us collapse in the desired direction. Furthermore, a bending actuator can be fabricated by adding a non-collapsing to one side of these actuators, as shown in Fig2.12. Finally, to show the non-planar capability of this method, a vase shape fiber reinforced structure was printed, as shown in Fig2.12-G.

Finally, as mentioned, path printing provides the possibility to create a hybrid structure. As such, we employed this technique to create a hybrid robotics hand where the robot's main body is fabricated out of 3D printed material, and the joint between the rigid segments are fiber-based joint that provides high load capacitance and has low bending stiffness. Furthermore, the same method is used to embed the fiber for cable-driven actuation. Hence, the fiber not only provides the hybrid interface but also provides the actuation in the robotics hands. The design of this hand is shown in Fig2.13.

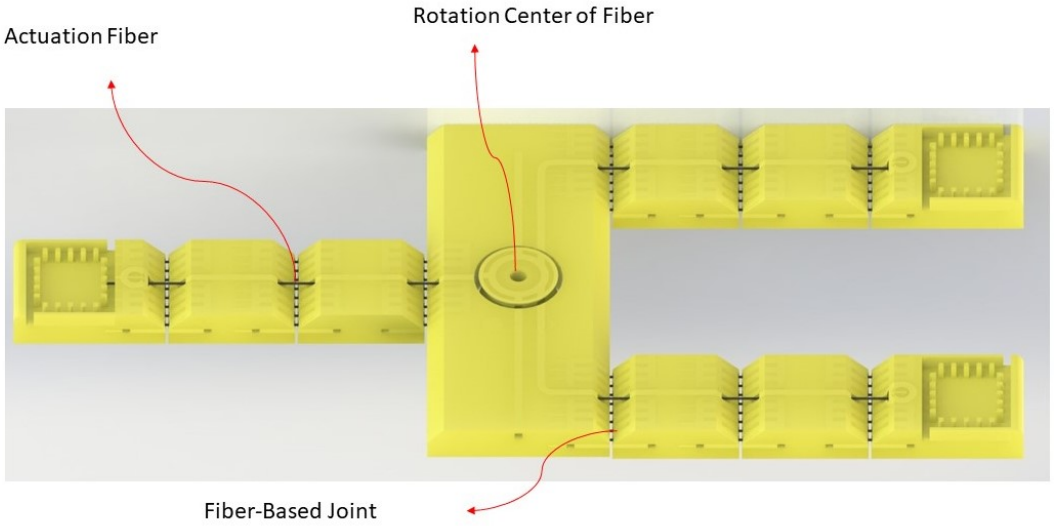

Figure 2.13: The model of 3D printed hand consists of fibre-based joints and fiber as acutation.

Chapter 3

Results

3.1 Fiber Reinforcement of Soft Robots

3.1.1 Two sided weaving patter

In this test, we measured the force versus the extensibility of the fiber-reinforced soft material and investigated how weaving parameters affect stiffness. We performed this experiment for various pins' distances and diameters over a certain distance. As shown in Fig3.1-(A), for two pins with a diameter of 2mm, the extensibility is relatively low due to the pattern, and the composite would strain 7.2% under 2MPa stress. By increasing the number of pins with the same diameter of 2mm, the extensibility of the structure increases; thus, the stiffness is smaller at lower strains. For the four pins 2mm, the stiffness is low until 1.66 % strain, and for six pins, the extensibility range increases to 6% of the strain. Furthermore, we repeated the test for the different pins' diameters while keeping the number of pins to 4. As demonstrated in Fig3.1, increasing the diameter of pins increases the extensibility. For pins with a diameter of 2mm, the stress reaches to 0.5MPa at 4.2% strain, while for 3mm, 4mm, and 5mm, the strain number is respectively 5.5%, 8.6%, and 15.3%. This result shows how stiffness and extensibility can be easily controlled for various applications by changing the distance and diameter. Finally, we also repeated the test for the same sample without fiber reinforcement. As expected, the stiffness of Ecoflex 00-10 is significantly lower than fiber-reinforced structures. The Ecoflex reached 0.3 MPa at 600% strain which is considerably more extensible compared to fiber-reinforced structures.

Furthermore, we conducted another test to demonstrate the resilience of the fiber-reinforced structure, this time using the 4 pins with 2mm diameter under 1000 cycles of 200N cyclic load. As shown in Figure 3.1-(B), the results indicate that the fiber structure is highly repeatable under cyclic force, with less than 5% change observed over 1000 cycles. These findings suggest that the fiber-reinforced structure can withstand repeated stress and maintain its stability and performance over time.

3.1.2 One side Serpentine

In addition to the pins' diameter, we performed an experiment to investigate the effect of the serpentine pattern and how the density of pins over a certain distance can control the material's stiffness. As demonstrated in Fig3.1-(C), the stiffness of a sample with three pins is higher than in other cases. The soft material with three pins stretches around 50% of its length while requiring 0.6MPa. However, the sample with 5, 7, and 9 pins are less than 0.2 MPa at higher strains. In addition, 7

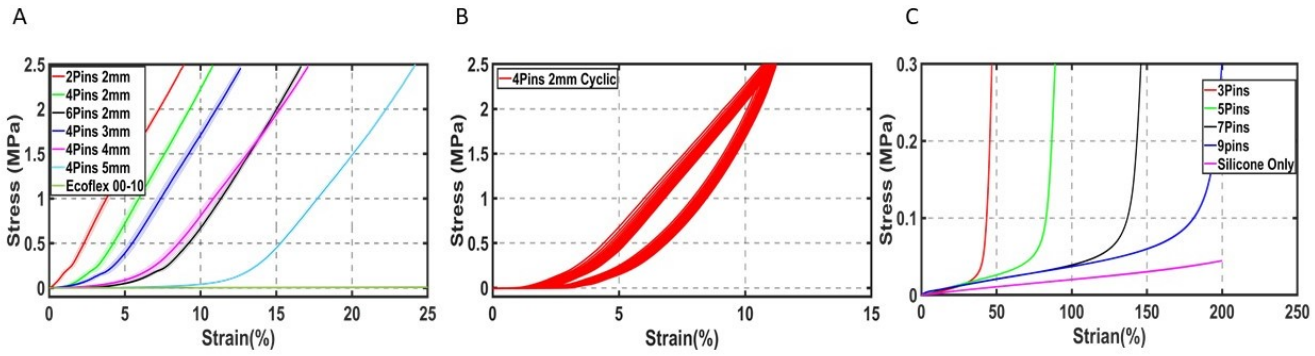

Figure 3.1: The experimental result on the extensibility of the fiber reinforced structure, (A) the test result on stress vs strain of two-sided pattern for different numbers of pins and different diameters. (B) The cyclic test of 4pins with 2mm diameter and the resilience of the structure (C) The stiffness test of serpentine shape for different numbers of pins

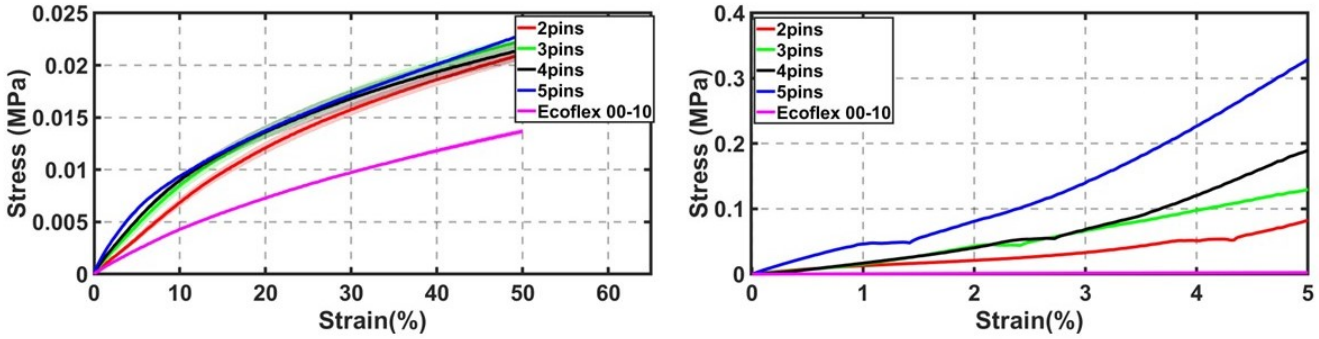

Figure 3.2: The vertical stiffness test for samples with and without vertical fibers. (A) effect of having reinforcement in the other direction on vertical stiffness. (B) effect of increasing the number of vertical fibers in vertical stiffness.

and 9 pins are nearly identical, requiring 34KPa and 31KPa to be extended 100% of their length. Finally, we performed the test on a sample with just Ecoflex 00-10, and as expected, the stiffness is lower than in other cases.

3.1.3 Vertical Fiber

In this experiment, we investigated the effect of vertical fibers on vertical stiffness. First, we performed the experiment on samples shown in Fig3.2-(A) without having vertical fibers. As presented, The fiber reinforcement in one direction increases the stress required for 50% strain from 14KPa to 23KPa for a sample with five pins; thus, the fiber reinforcement increases the stiffness in other directions as well. In addition, we observed that increasing the number of pins, even without having vertical fibers, increases the vertical stiffness slightly, as presented from 0.021 for two pins to 0.023MPa for five pins.

In the next step, we added the vertical fibers to the sample and repeated the test only until 5% strain since the vertical fibers prevent additional extensions. The result presented in Fig3.2-B shows that, as expected, adding vertical fiber increases the vertical stiffness significantly from 6KPa to 80KPa with only two vertical fibers at 5% strain. Furthermore, adding more vertical fibers strengthen the stiffness as the structure with five vertical fibers requires 0.329 MPa, while it is 0.187MPa for four pins and 0.128MPa for three pins.

3.1.4 Pins Bending Test

As mentioned in 2.3.3, we used four different materials as our loom. Each of these materials provides specific properties in the process and can be beneficial for different applications. Moreover, due to the mechanical properties of these materials, they behave differently under the shear force created by fiber tension. For example, as presented in Table3.1, the PLA has the highest breaking point with 60.72 N at 0.91 mm compression. After that, PVA has the second-highest breaking force, with 50.89 N at 0.75mm. Finally, the layfomm 00-40 before washing with water and PET has 16.76N and 9.12N, respectively.

Table 3.1: Pin materials used in weaving process with functionality and limitations of each material

Pin Material	Breaking Load	Functionality	Limitation
PLA	60.72N	High Strength, Straightforward Print	Removing after deposition
PVA	50.89N	Water Soluble	Brittle, Oozing, Difficulty in Print
Layfomm	16.76N	Flexibility after washing, Vertical Fiber	Oozing, Difficulty in print, Low shear force tolerance
PET	9.12N	Straightforward print, High axial strength	Low shear force tolerance, Removing after deposition

3.1.5 Prototypes

We fabricated various actuators to show the wide range of patterns and possibilities that our proposed method can create. First, we created an extending actuator by just radially reinforcing a silicone rubber structure using a pattern shown in section 3.3. In this actuator, the radial reinforcement prevents expansion in that direction, and softness in the axial direction leads to extension. This actuator could be inflated until 0.8 bar of relative pressure, extending nearly 50% of the initial length from 5mm to 7.5mm. Furthermore, we added multiple vertical fibers on one side of the actuator using straw weaving. Adding these two vertical fibers to the extending actuator changes the deformation to bending (Fig3.3). In this actuator, under the same pressure as extending, the bending actuator bends 180°.

In another design, we twisted the looms' pins and weaved around them to create a twisting actuator. This actuator can twist nearly 120 ° by applying 0.9 bar of relative pressure. This actuator is a prime example of an actuator that is not possible to fabricate using the current automatized methods and printing the loom and head changing enables such patterns.

Finally, regarding the vacuum actuators, first, the contraction actuator shown in Fig3.3-(A) was able to lift a 500-gram weight nearly 20 times its weight. In addition, the second contraction actuator was able to lift 100 grams, nine times its weight. Finally, the vacuum bending actuator bends nearly 90°. However, the provided stiffness was significantly lower compared to the pressure actuator.

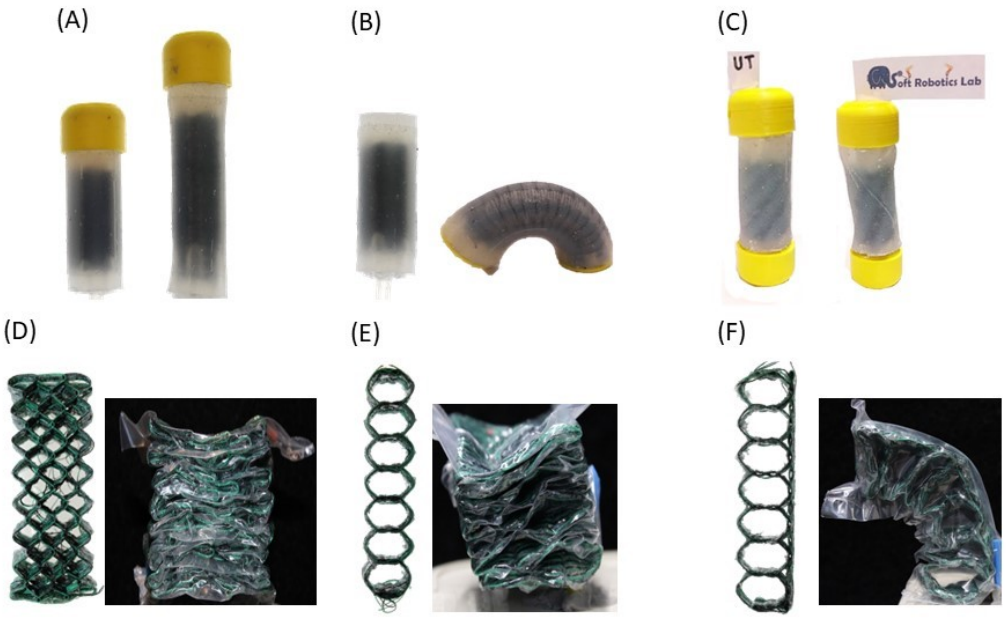

Figure 3.3: Different inflatable and vacuum actuators fabricated using the proposed weaving technique. (A) Extension actuator, (B) Inflatable bending actuator, (C) Twisting actuator, (D)(E) contraction actuator, (F) vacuum bending actuator

3.2 Hybrid Hand Gripper

3.2.1 Printing Parameter Axial Test

As explained in 2.3.6, first, we experimented on different extrusion rates to find which percentage provided the best bonding between fiber and PLA. As shown in Fig3.4, the lowest recorded force was 14.61N at 20%, and the highest recorded was 54.93N at 120%. The main trend in this experiment shows, as expected, increasing the extrusion to 120% improves the axial load capacity. However, increasing from 120% to 140% decreases the breaking force to 48.53N.

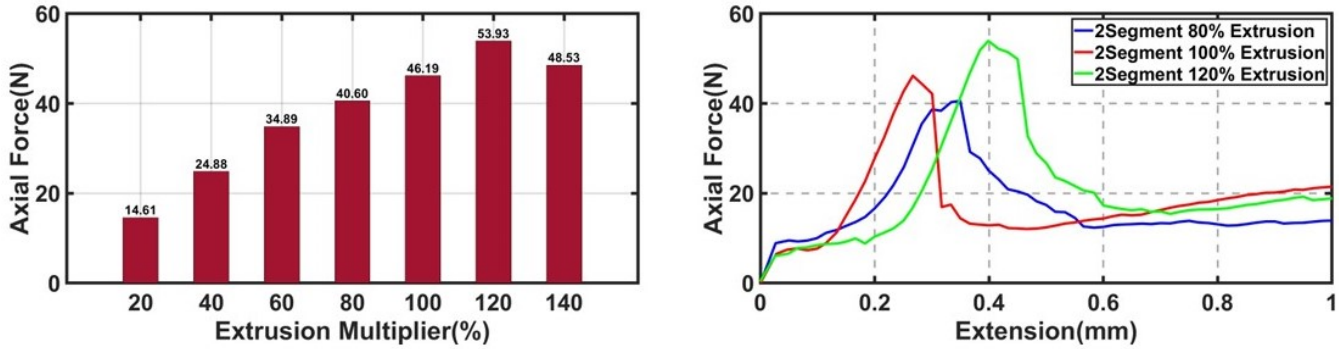

Figure 3.4: The Axial Load capacity of the hybrid hinge with different extrusion rates. (A) The maximum recorded force vs the extrusion rate. (B) The axial force vs extension force for different 80%, 100%, 120%

In the second experiment, we increased the number of slots to observe how this parameter affects the axial load capacity. As demonstrated in Fig3.5, as expected, increasing the number of slots raises the axial load capacity from 46.19N in 2 slots to 88.71N for 5 slots.

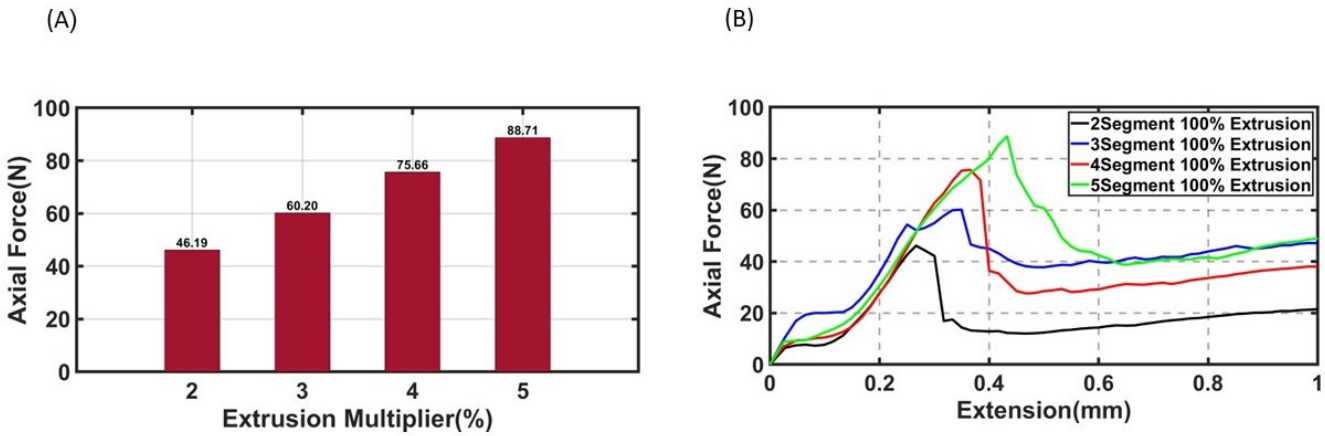

Figure 3.5: The Axial Load capacity of hybrid joint with different numbers of slots. (A) The maximum recorded force vs the number of slots. (B) The axial force vs extension force different slot number

3.2.2 Joint Comparison

To compare the performance of our gripper joint with currently available 3D-printed soft joints, we conducted axial and 3D point bending tests on a fiber-based joint, a 2mm 3D-printed Ninjaflex joint, and a 0.5mm Ninjaflex joint with the same thickness as the fiber hinge. As depicted in Fig3.6, the fiber joint demonstrated a remarkable ability to withstand axial forces of up to approximately 400N, whereas the 2mm Ninjaflex joint yielded at nearly 100N. As anticipated, the 0.5mm Ninjaflex sample had a lower yield point at 25N.

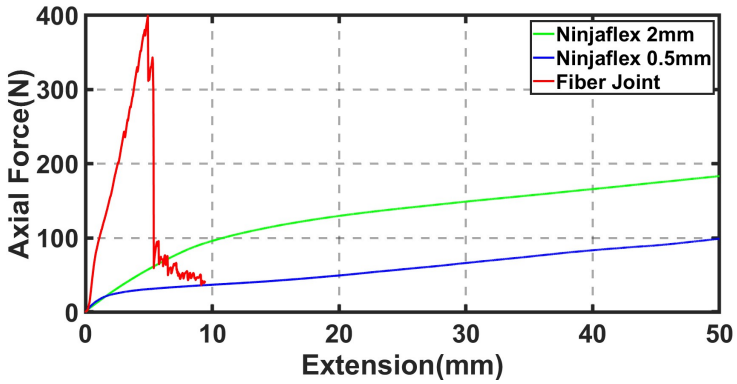

Figure 3.6: The Axial Load capacity of the hybrid joint in comparison with previously designed hinges proposed in [55].

Furthermore, as shown in Fig3.7, the forces recorded from the 3D point bending test of the fiber joint are less than 0.04N, which can be assumed zero compared to the usual robotics joint bending forces. This value, however, is significantly higher for a 2mm Ninjaflex join since it requires nearly 120 times more force to be bent 90°.

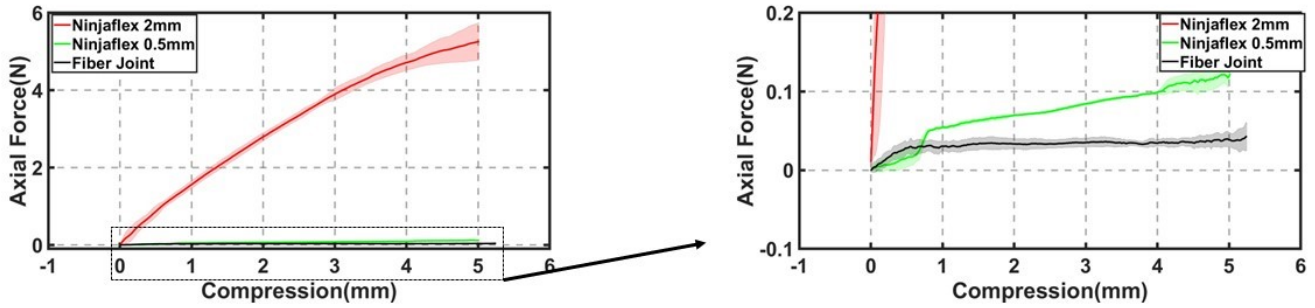

Figure 3.7: The 3D point bending test of the fiber-based hybrid hinge in comparison with TPU Ninjaflex hinge with 0.5mm and 2mm thickness.

3.2.3 Hybrid Hand Gripper

We have demonstrated the versatility of the proposed method for creating hybrid structures by utilizing path printing to fabricate a hybrid hand gripper. As illustrated in Fig3.8, this hand is capable of effortlessly adapting to objects that need to be grasped, thanks to the low bending stiffness of the fiber-based joint. Moreover, the rigid body of the hand offers high lateral stiffness, which is not attainable with conventional soft actuators without requiring additional stiffness modulation.

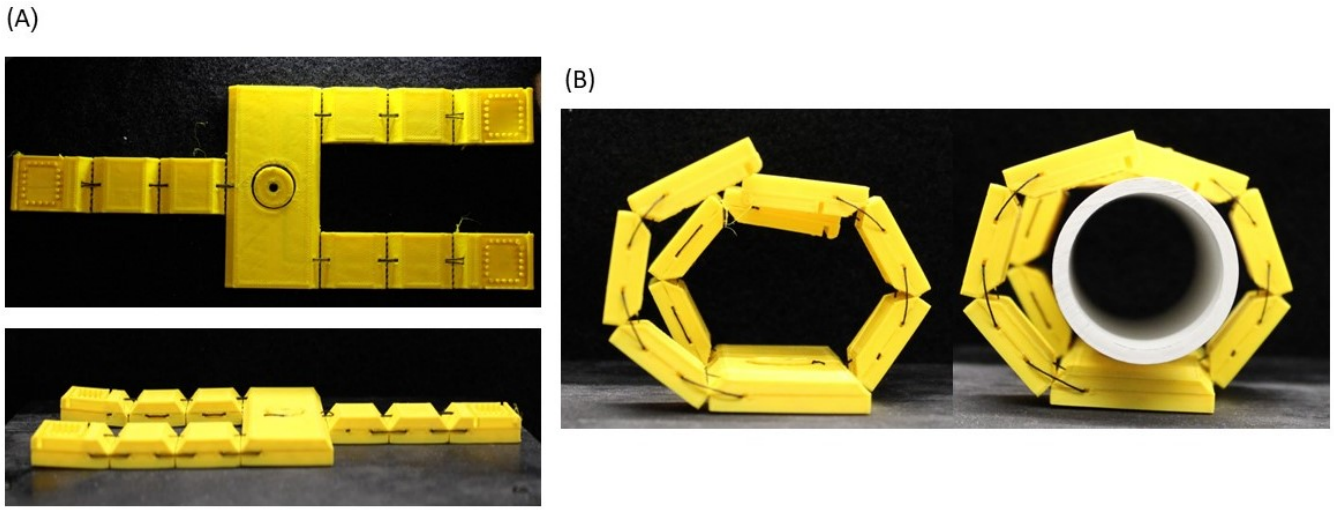

Figure 3.8: The 3D printed hybrid hand with cable driven actuation. (A) the hand before actuation. (B) the hand after actuation, grasping a pipe and easily adapting to the pipe.

3.2.4 Bonding to soft material

We utilized fiber reinforcement to mimic the behavior of connective tissues and facilitate bonding between a 3D-printed rigid structure and soft rubber(2.3.6). To evaluate the effectiveness of the fiber interface, we conducted a lap shear bonding test on samples resembling the one shown in Fig2.11. As a point of comparison, we also conducted the same experiment on a sample using glue. As depicted in Fig3.9, the bonding between the silicone and PLA materials failed at 7.31N when using silicone glue, while the use of three pins of fiber reinforcement resulted in a bonding strength of 9.01N. However, when the number of pins was increased from 4 to 6, the bonding strength decreased from 8.72N to

7.50N.

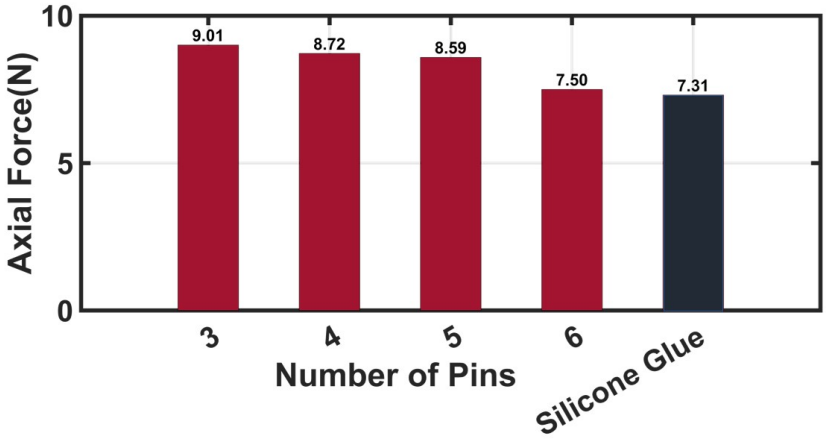

Figure 3.9: The lap shear test results between silicone rubber and PLA using both fiber interface and glue.

Finally, to demonstrate the practical application of bonding between silicone rubber and 3D-printed thermoplastic, we printed a structure resembling bone and muscle (Fig3.10). The design consisted of a 3D-printed core in the center representing the bone, with multiple fibers woven around it to serve as bonding points for the silicone structure mimicking the muscle. Without the fibers, the silicone would easily detach from the PLA core.

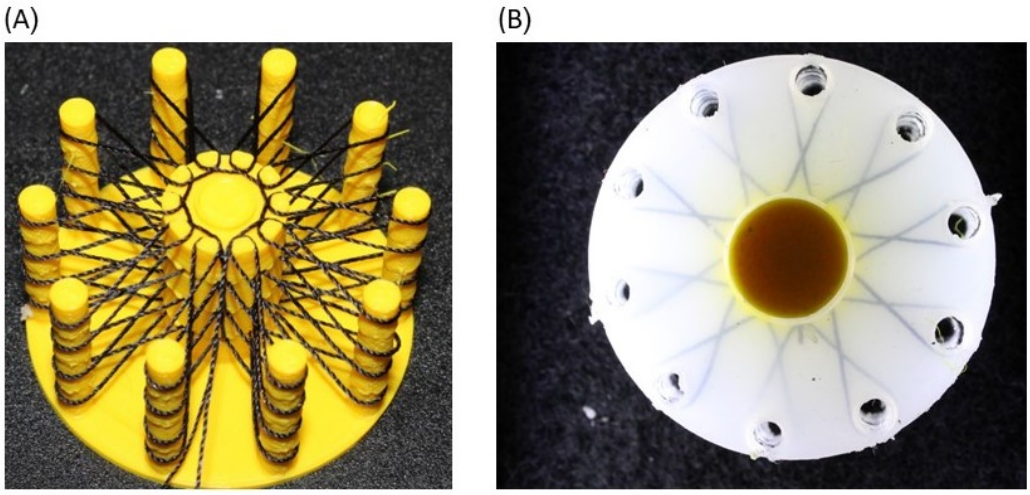

Figure 3.10: A prototype to mimic bone and muscle structure with fiber as connective tissue (A) the woven structure on the printer before casting (B) the structure after the casting.

Chapter 4

Discussion

4.1 3D weaving of Soft actuators

This report describes a novel fabrication technique that improves upon previously developed weaving methods in soft robotics [36] by allowing for 3D printing and non-planar structures. By employing a tool-changing and printing loom, and weaving fibers iteratively, the dimensions of the loom can be reduced by using shorter and thinner needles. Our technique can print textiles with a resolution of 1 end per inch and a height of 40mm. Additionally, the ability to pause during printing allows for the possibility of weaving fibers around twisted pins, as demonstrated in the twisting actuator. This technique greatly expands the possible patterns and geometries that can be used to integrate fibers into soft materials and control their stiffness to achieve desired deformations and behaviors..

We conducted two experiments to evaluate the stiffness and extensibility of our 3D-printed loom and serpentine pattern. In the first experiment, we used a two-sided pattern and varied the pins' diameter and number to characterize the stiffness. As shown in Fig3.1-(A), increasing the diameter and number of pins increased the extensible range, in agreement with Eq2.2. Surprisingly, the stiffness of all scenarios was higher than Ecoflex 00-10, contrary to our expectation that it would be similar in the extensible range. The stiffness of the second part, mostly due to the fiber stiffness, aligned with Eq2.5.

In the second experiment, we used a serpentine pattern to demonstrate how our method can achieve different stiffness and extensibility. Consistent with Eq2.3, increasing the number of pins and fiber length increased the extensibility. For example, the extensible range was less than 40% for three pins, while it surged to 70% for five pins, and the stiffness was similar to Ecoflex 00-10 for seven and nine pins over the measured strain. Moreover, the serpentine pattern provided significantly less stiffness than the two-sided pattern in all scenarios.

On another point, since our technique allows adding vertical fiber, we experimented with the effect of vertical fiber on stiffness. While experimenting on samples without vertical fiber, the results unexpectedly reveal that even without adding the vertical fibers, the fiber reinforcements enhance the stiffness in the other direction(Fig3.2). One possibility for this phenomenon can be that each layer of woven fiber during stretching behaves as a short fiber reinforcement in the non-reinforced structure and improve the stiffness. Moreover, as expected, adding vertical fiber remarkably changes the mechanical properties, and adding more vertical fibers increases will further increase the stiffness. Combining this result with the previous experiment shows that although finer fiber leads to more extensibility in one direction, it improves the inextensibility in another direction.

Moreover, we investigated four different materials as printing pins. Each of these materials provides specific properties that can be advantageous in some applications. However, in all cases, as shown in Fig4.1, the fibers, especially in the corners, apply significant shear force due to the capstan effect that may lead to a deflection of the pins or break in the pins. Therefore, we performed a bending test to show which material suits to avoid this problem. As illustrated in Table3.1, the PLA has the highest bending resistance, and layfomm provides the most significant deflection before breaking. One interesting point is that PET surprisingly breaks at a lower force than all other materials despite its higher tensile strength compared to other materials. The reason behind this low shear force resistance is the low bending flexural stiffness of the PET compared to PLA, which is 1/4 of PLA. One possible solution to avoid shortcomings due to the low bending stiffness of the material is active fiber tension control and path planning to avoid tensions at specific pins without losing the required tension for the structure. In addition, in table 3.1, the benefits and disadvantages of each of these materials are written as a comparison.

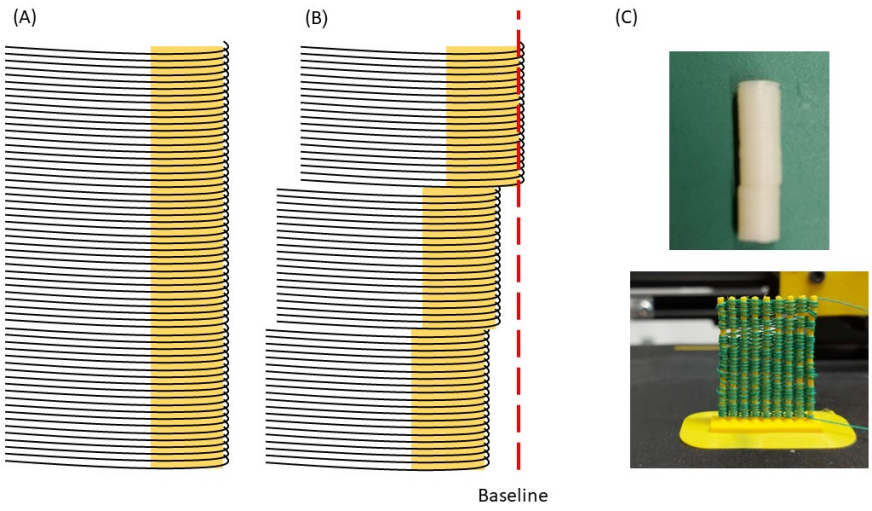

Figure 4.1: The layer shift happens due to the capstan effect of fibers on the pins, especially on the corner pins. (A) the desired final pattern (B) The layer shift due to fiber tension and no proper path planning. (C) the actual misalignment in the location of the pin.

As a final point of discussion, we showed that it is possible to weave complex and non-planar structures using this technique, such as angular structures(Fig4.2). However, there is a limitation in the patterns that can be generated with our method. During weaving around angular pins, we observed that after a certain angle, the friction between the fiber and the pins is insufficient, and the fiber slides over the angular pins. These critical angles differed depending on the layer height, printing quality, and speed. However, on average, this angle is 30°. As such, printing, especially with a convex angular pin, is not possible for all angles with the current method. As a solution, grooves can be printed on the pins so the fibers be placed inside these grooves as shown in Fig4.2-(B). However, these grooves reduce the fiber density in the Z-direction. Moreover, the size and fineness of the grooves depend heavily on the printing parameters and affect the process. Another solution is to contaminate the fiber with an adhesive so it can attach to the pins' surface and prevent slippage.

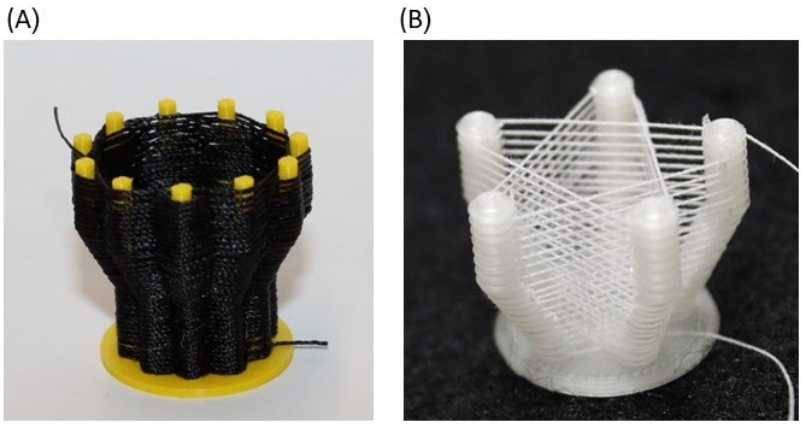

Figure 4.2: Non planar 3D weaving of a vase. (A) the fibers are woven around the pins; however, at a certain angle, they start to slip on the pins (B) Using grooves on the pins to predefine the position of the fibers. However, to be able to take off the pins later, the pins in the second method should be made of PVA.

4.2 Fiber-based Hybrid Robot

In addition to weaving fiber structures for soft robotics applications, this report presents a new method to create hybrid structures and bond to the thermoplastic substrate. Due to the high axial strength, simultaneously having very low bending stiffness, and direct bonding to the 3D printing substrate, the fibers provide a great solution to create a fiber-based joint for hybrid robotics applications.

Therefore, we first experimented with various scenarios, such as the extrusion rate in the path cavity and the number of axial fibers, to find the best parameters to have the best bonding and highest axial strength. As shown in Fig3.4, by increasing the extrusion multiplier from 20% to 120%, the axial force required to debond the fiber from the PLA substrate increases significantly. This result is anticipated since in 20%, the fibers are not encapsulated properly by the PLA. Furthermore, after 140%, the debonding force decreases from 53.93N to 48.53N. The reason behind this decrease can be that the PLA fills the slot similarly to 120%. However, the high temperature of the extra filaments may affect the bonding between PLA layers since the PLA is injected at the cavity at a much higher temperature than the average printing temperature (230°C to 205°C). Moreover, the extension value shows that the fibers and PLA remain bonded only before 0.4mm extension, due to the inextensibility of both fiber and PLA.

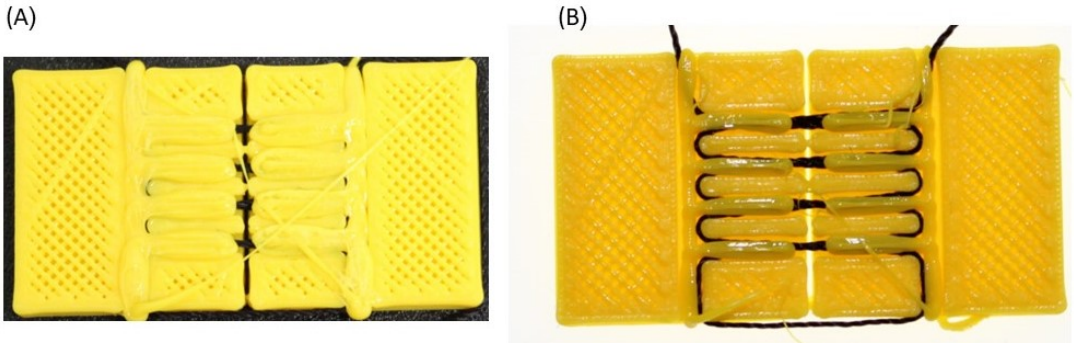

Figure 4.3: Fiber encapsulation and embedding with different extrusion multipliers, (A) with 100% which barely embed the fiber, (B) with 20% that fill the cavity.

In addition, we increased the number of path sloths from 2 to 5 with a 100% extrusion rate. As expected, since the length of the encapsulated fiber is increased, thus the friction point between the fiber and PLA is increased. In this experiment, by increasing the number of sloths, the breaking point also moves from 0.25mm to 0.45mm due to higher entanglement between PLA and nylon fiber.

After optimizing and finding the trends in bonding between PLA and fiber, we compare the developed joint to the conventional flexible thermoplastic (Ninjaflex, shore hardness 85A). The result in Fig3.6 shows that the fiber joint, despite the small thickness, provides much better axial strength than even 2mm Ninjaflex which is mostly used to fabricate soft fingers. Moreover, despite high axial force compared to Ninjaflex (400N to 100N for 2mm and 25N for 0.5mm), the fibers joint bend with forces less than 0.03N, which is nearly 150 times less than 2mm Ninjaflex.

Finally, the prototype in Fig3.8 demonstrates that the fiber not only can work as a very efficient joint but the fiber can also have functionality such as actuation. In the future, conductive fibers can be used to integrate the sensor inside the fabricated hand.

As a final part of this work, we used the fibers to connect PLA and Silicone rubber. The results in Fig3.9 show that the fiber provides a better bonding solution than the glue in all scenarios. However, although we expected increasing the number of pins and, as a result having a finer fiber grip to enhance the bonding properties, the results show that increasing the pins reduces the bonding strength. One possible explanation for such observation is that the pins on one side of the silicone rubber work as a stress point, as shown in Fig4.4, and increasing the number of pins increased these stress concentration and weak points and results in earlier failure.

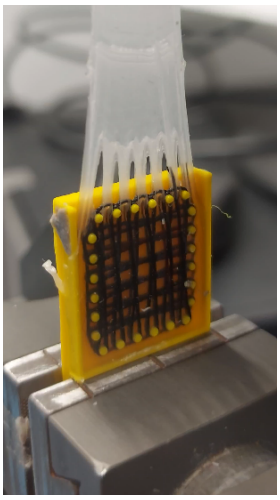

Figure 4.4: The moment the silicone rubber debonds from the pins and the pins cavities leads to weak points in silicone rubber and lower force tolerance.

Chapter 5

Conclusions

This study proposes a novel automated fabrication method for fiber-based structures in robotics. Our approach not only enables the creation of 3D complex fiber structures for soft robots, which is cumbersome and time-consuming when done manually but also allows for the bonding of fiber with rigid materials to create hybrid robotics systems. To achieve this, we modified a conventional FDM printer to print the path or loom and then weave the fiber around it.

In the initial phase of this study, FDM was utilized to print a pin and weave the fiber around the loom. This innovative approach offers a high level of flexibility in controlling the stiffness of soft materials, as well as the ability to fabricate non-planar structures that are not feasible using conventional methods. This technique also allows for the production of finer textiles and the creation of 3D soft robotic designs, which represents a significant advancement in the field. Finally, a wide range of inflatable and vacuum-based actuators with complex behavior was fabricated to demonstrate how beneficial this method can be in the fabrication of soft robots.

Moreover, we explored a novel hybrid design for a robotic hand gripper that resolves the issue of high bending stiffness in rigid robots and overcomes the axial load capacity limitation of soft joints. Additionally, we investigated the fiber embedding technique as a possible solution to overcome the limitation of bonding between rigid and soft structures.

In summary, this innovative fiber embedding technique opens up new possibilities for research in the field of soft robotics and holds great potential for the fabrication of next-generation soft and hybrid robots.

5.1 Future Work

Regarding future work, one possible enhancement to the current process could be to automate vertical fiber embedding. There are several possibilities for achieving this, including using soft materials for the pins, employing different techniques such as Z-pinning to add the vertical fiber at a later stage, or developing a mechanism to pull fibers inside the pins. Additionally, encapsulating the fibers within the soft matrix would be a crucial step toward full automation, eliminating the need to deposit or cast the soft material after weaving. Furthermore, the stickiness of such materials helps hold the fibers, particularly for angular pins.

Furthermore, in this work, we mainly focus on the bonding between PLA and fiber, as well as the bonding between silicone to PLA via fiber interface. One interesting aspect of future work can be

the usage of conductive fibers in the hybrid hands' structure to bring more functionality, such as sensing or power transmission, to the structure.

References

[1] D. Rus and M. Tolley, "Design, fabrication and control of soft robots," *Nature*, vol. 521, pp. 467–75, 05 2015.

[2] J. Hughes, U. Culha, F. Giardina, F. Guenther, A. Rosendo, and F. Iida, "Soft manipulators and grippers: A review," *Frontiers in Robotics and AI*, vol. 3, 11 2016.

[3] E. Brown, N. Rodenberg, J. Amend, A. Mozeika, E. Steltz, M. Zakin, H. Lipson, and H. Jaeger, "Universal robotic gripper based on the jamming of granular material," *Proceedings of the National Academy of Sciences of the United States of America*, vol. 107, 10 2010.

[4] T. Ranzani, G. Gerboni, M. Cianchetti, and A. Menciassi, "A bioinspired soft manipulator for minimally invasive surgery," *Bioinspiration amp Biomimetics*, vol. 10, 03 2015.

[5] J. Kim, Y. Nakajima, and K. Kobayashi, "A suction-fixing, stiffness-tunable liver manipulator for laparoscopic surgeries," *IEEE/ASME Transactions on Mechatronics*, vol. 23, no. 1, pp. 262–273, 2018.

[6] C. M. Thalman, Q. P. Lam, P. H. Nguyen, S. Sridar, and P. Polygerinos, "A novel soft elbow exosuit to supplement bicep lifting capacity," in *2018 IEEE/RSJ International Conference on Intelligent Robots and Systems (IROS)*, 2018, pp. 6965–6971.

[7] K. Leibrandt, P. Wisanuvej, G. Gras, J. Shang, C. Seneci, P. Giataganas, V. Vitiello, A. Darzi, and G.-Z. Yang, "Effective manipulation in confined spaces of highly articulated robotic instruments for single access surgery," *IEEE Robotics and Automation Letters*, vol. PP, pp. 1–1, 02 2017.

[8] B. Mazzolai, A. Mondini, F. Tramacere, G. Riccomi, A. Sadeghi, G. Giordano, E. Del Dottore, M. Scaccia, M. Zampato, and S. Carminati, "Octopus-inspired soft arm with suction cups for enhanced grasping tasks in confined environments," *Advanced Intelligent Systems*, vol. 1, no. 6, p. 1900041, 2019. [Online]. Available: https://onlinelibrary-wiley-com.ezproxy2.utwente.nl/doi/abs/10.1002/aisy.201900041

[9] T. George Thuruthel, Y. Ansari, E. Falotico, and C. Laschi, "Control strategies for soft robotic manipulators: A survey," *Soft Robotics*, vol. 5, no. 2, pp. 149–163, 2018, pMID: 29297756. [Online]. Available: https://doi.org/10.1089/soro.2017.0007

[10] C. Laschi, M. Cianchetti, B. Mazzolai, L. Margheri, M. Follador, and P. Dario, "Soft robot arm inspired by the octopus," *Advanced Robotics*, vol. 26, no. 7, pp. 709–727, 2012. [Online]. Available: https://doi.org/10.1163/156855312X626343

[11] E. Brown, N. Rodenberg, J. Amend, A. Mozeika, E. Steltz, M. R. Zakin, H. Lipson, and H. M. Jaeger, "Universal robotic gripper based on the jamming of granular material," *Proceedings of the National Academy of Sciences*, vol. 107, no. 44, pp. 18 809–18 814, 2010.

[12] M. Cianchetti, C. Laschi, A. Menciassi, and P. Dario, "Biomedical applications of soft robotics," *Nature Reviews Materials*, vol. 3, no. 6, pp. 143–153, 2018.

[13] J. Kaufmann, "New materials for sports equipment made of anisotropic fiber-reinforced plastics with stiffness related coupling effect," *Procedia engineering*, vol. 112, pp. 140–145, 2015.

[14] L. Mishnaevsky, K. Branner, H. N. Petersen, J. Beauson, M. McGugan, and B. F. Sørensen, "Materials for wind turbine blades: An overview," *Materials*, vol. 10, no. 11, 2017. [Online]. Available: https://www.mdpi.com/1996-1944/10/11/1285

[15] C. Soutis, "Carbon fiber reinforced plastics in aircraft construction," *Materials Science and Engineering: A*, vol. 412, no. 1-2, pp. 171–176, 2005.

[16] P. K. Mallick, *Fiber-reinforced composites: materials, manufacturing, and design*. CRC press, 2007.

[17] M. A. Freilich, J. P. Duncan, E. K. Alarcon, K. A. Eckrote, and A. J. Goldberg, "The design and fabrication of fiber-reinforced implant prostheses," *The Journal of prosthetic dentistry*, vol. 88, no. 4, pp. 449–454, 2002.

[18] F. Connolly, C. J. Walsh, and K. Bertoldi, "Automatic design of fiber-reinforced soft actuators for trajectory matching," *Proceedings of the National Academy of Sciences*, vol. 114, no. 1, pp. 51–56, 2017. [Online]. Available: https://www.pnas.org/doi/abs/10.1073/pnas.1615140114

[19] P. H. Nguyen and W. Zhang, "Design and computational modeling of fabric soft pneumatic actuators for wearable assistive devices," *Scientific reports*, vol. 10, no. 1, p. 9638, 2020.

[20] S. P. M. Babu, A. Sadeghi, A. Mondini, and B. Mazzolai, "Antagonistic pneumatic actuators with variable stiffness for soft robotic applications," in *2019 2nd IEEE International Conference on Soft Robotics (RoboSoft)*, 2019, pp. 283–288.

[21] K. Suzumori, S. Iikura, and H. Tanaka, "Development of flexible microactuator and its applications to robotic mechanisms," in *Proceedings. 1991 IEEE International Conference on Robotics and Automation*, 1991, pp. 1622–1627 vol.2.

[22] K. Suzumori, S. Endo, T. Kanda, N. Kato, and H. Suzuki, "A bending pneumatic rubber actuator realizing soft-bodied manta swimming robot," in *Proceedings 2007 IEEE International Conference on Robotics and Automation*, 2007, pp. 4975–4980.

[23] E. T. Roche, R. Wohlfarth, J. T. B. Overvelde, N. V. Vasilyev, F. A. Pigula, D. J. Mooney, K. Bertoldi, and C. J. Walsh, "A bioinspired soft actuated material," *Advanced Materials*, vol. 26, no. 8, pp. 1200–1206, 2014. [Online]. Available: https://onlinelibrary-wiley-com.ezproxy2.utwente.nl/doi/abs/10.1002/adma.201304018

[24] F. B. Coulter, M. Schaffner, J. A. Faber, A. Rafsanjani, R. Smith, H. Appa, P. Zilla, D. Bezuidenhout, and A. R. Studart, "Bioinspired heart valve prosthesis made by silicone additive manufacturing," *Matter*, vol. 1, no. 1, pp. 266–279, 2019. [Online]. Available: https://www.sciencedirect.com/science/article/pii/S2590238519300384

[25] J. H. Pikul, S. Li, H. Bai, R. T. Hanlon, I. Cohen, and R. F. Shepherd, "Stretchable surfaces with programmable 3d texture morphing for synthetic camouflaging skins," *Science*, vol. 358, no. 6360, pp. 210–214, 2017. [Online]. Available: https://www.science.org/doi/abs/10.1126/science.aan5627

[26] L. Lan, C. Jiang, Y. Yao, J. Ping, and Y. Ying, "A stretchable and conductive fiber for multi-functional sensing and energy harvesting," *Nano Energy*, vol. 84, p. 105954, 2021.

[27] D. Hardman, T. George Thuruthel, A. Georgopoulou, F. Clemens, and F. Iida, "3d printable soft sensory fiber networks for robust and complex tactile sensing," *Micromachines*, vol. 13, no. 9, p. 1540, 2022.

[28] S. Jain, T. Stalin, E. Kanhere, and P. V. y. Alvarado, "Flexible fiber interconnects for soft mechatronics," *IEEE Robotics and Automation Letters*, vol. 5, no. 3, pp. 3907–3914, 2020.

[29] X. Li, S. Chen, Y. Peng, Z. Zheng, J. Li, and F. Zhong, "Materials, preparation strategies, and wearable sensor applications of conductive fibers: a review," *Sensors*, vol. 22, no. 8, p. 3028, 2022.

[30] A. R. Plamootil Mathai, T. Stalin, and P. Valvivia y Alvarado, "Flexible fiber inductive coils for soft robots and wearable devices," *IEEE Robotics and Automation Letters*, vol. 7, no. 2, pp. 5711–5718, 2022.

[31] X. Huang, K. Kumar, M. K. Jawed, A. Mohammadi Nasab, Z. Ye, W. Shan, and C. Majidi, "Highly dynamic shape memory alloy actuator for fast moving soft robots," *Advanced Materials Technologies*, vol. 4, no. 4, p. 1800540, 2019. [Online]. Available: https://onlinelibrary-wiley-com.ezproxy2.utwente.nl/doi/abs/10.1002/admt.201800540

[32] M. Gifari, H. Naghibi, S. Stramigioli, and M. Abayazid, "A review on recent advances in soft surgical robots for endoscopic applications," *The International Journal of Medical Robotics and Computer Assisted Surgery*, vol. 15, 05 2019.

[33] R. Wang, C. Zhang, W. Tan, J. Yang, D. Lin, and L. Liu, "Electroactive polymer-based soft actuator with integrated functions of multi-degree-of-freedom motion and perception," *Soft Robotics*, vol. 0, no. 0, p. null, 0, pMID: 35482290. [Online]. Available: https://doi.org/10.1089/soro.2021.0104

[34] A. Fannir, R. Temmer, G. T. M. Nguyen, L. Cadiergues, E. Laurent, J. D. W. Madden, F. Vidal, and C. Plesse, "Linear artificial muscle based on ionic electroactive polymer: A rational design for open-air and vacuum actuation," *Advanced Materials Technologies*, vol. 4, no. 2, p. 1800519, 2019. [Online]. Available: https://onlinelibrary-wiley-com.ezproxy2.utwente.nl/doi/abs/10.1002/admt.201800519

[35] A. Atalay, V. Sanchez, O. Atalay, D. M. Vogt, F. Haufe, R. J. Wood, and C. J. Walsh, "Batch fabrication of customizable silicone-textile composite capacitive strain sensors for human motion tracking," *Advanced Materials Technologies*, vol. 2, no. 9, p. 1700136, 2017. [Online]. Available: https://onlinelibrary-wiley-com.ezproxy2.utwente.nl/doi/abs/10.1002/admt.201700136

[36] T. Stalin, N. Thanigaivel, V. Joseph, and P. V. Alvarado, "Automated fiber embedding for tailoring mechanical and functional properties of soft robot components," in *2019 2nd IEEE International Conference on Soft Robotics (RoboSoft)*, 2019, pp. 762–767.

[37] K. Galloway, K. Becker, B. Phillips, J. Kirby, S. Licht, R. Wood, and D. Gruber, "Soft robotic grippers for biological sampling on deep reefs," *Soft Robotics*, vol. 3, 01 2016.

[38] R. Rahimi, W. Yu, M. Ochoa, and B. Ziaie, "Directly embroidered microtubes for fluid transport in wearable applications," *Lab on a Chip*, vol. 17, no. 9, pp. 1585–1593, 2017.

[39] F. Daerden, D. Lefeber *et al.*, "Pneumatic artificial muscles: actuators for robotics and automation," *European Journal of Mechanical and Enviromental Engineering*, vol. 47, no. 1, pp. 11–22, 2002.

[40] D. Sangian, A. Jeiranikhameneh, S. Naficy, S. Beirne, and G. M. Spinks, "Three-dimensional printed braided sleeves for manufacturing mckibben artificial muscles," *3D Printing and Additive Manufacturing*, vol. 6, no. 1, pp. 57–62, 2019. [Online]. Available: https://doi.org/10.1089/3dp.2018.0103

[41] Y. Luo, K. Wu, A. Spielberg, M. Foshey, D. Rus, T. Palacios, and W. Matusik, "Digital fabrication of pneumatic actuators with integrated sensing by machine knitting," in *Proceedings of the 2022 CHI Conference on Human Factors in Computing Systems*, 2022, pp. 1–13.

[42] Y. Sun, J. Guo, T. M. Miller-Jackson, X. Liang, M. H. Ang, and R. C. H. Yeow, "Design and fabrication of a shape-morphing soft pneumatic actuator: Soft robotic pad," in *2017 IEEE/RSJ International Conference on Intelligent Robots and Systems (IROS)*, 2017, pp. 6214–6220.

[43] V. Sanchez, C. J. Walsh, and R. J. Wood, "Textile technology for soft robotic and autonomous garments," *Advanced Functional Materials*, vol. 31, no. 6, p. 2008278, 2021. [Online]. Available: https://onlinelibrary.wiley.com/doi/abs/10.1002/adfm.202008278

[44] O. Sosanya, "Oluwaseyi sosanya's 3d weaving machine." https://www.sosafresh.com/3d-weaver/, accessed: 2023-02-23.

[45] M. Schaffner, J. A. Faber, L. Pianegonda, P. A. Rühs, F. Coulter, and A. R. Studart, "3d printing of robotic soft actuators with programmable bioinspired architectures," *Nature communications*, vol. 9, no. 1, pp. 1–9, 2018.

[46] N. W. Bartlett, M. T. Tolley, J. T. B. Overvelde, J. C. Weaver, B. Mosadegh, K. Bertoldi, G. M. Whitesides, and R. J. Wood, "A 3d-printed, functionally graded soft robot powered by combustion," *Science*, vol. 349, no. 6244, pp. 161–165, 2015. [Online]. Available: https://www.science.org/doi/abs/10.1126/science.aab0129

[47] F. Lotti, P. Tiezzi, G. Vassura, and A. Zucchelli, "Mechanical structures for robotic hands based on the " compliant mechanism " concept," 2002.

[48] V. Megaro, J. Zehnder, M. Bächer, S. Coros, M. Gross, and B. Thomaszewski, "A computational design tool for compliant mechanisms," *ACM Trans. Graph.*, vol. 36, no. 4, jul 2017. [Online]. Available: https://doi-org.ezproxy2.utwente.nl/10.1145/3072959.3073636

[49] L. Rossing, R. B. Scharff, B. Chömpff, C. C. Wang, and E. L. Doubrovski, "Bonding between silicones and thermoplastics using 3d printed mechanical interlocking," *Materials & Design*, vol. 186, p. 108254, 2020.

[50] P. Kannus, "Structure of the tendon connective tissue," *Scandinavian Journal of Medicine & Science in Sports*, vol. 10, no. 6, pp. 312–320, 2000. [Online]. Available: https://onlinelibrary-wiley-com.ezproxy2.utwente.nl/doi/abs/10.1034/j.1600-0838.2000.010006312.x

[51] T. K. Borg and J. B. Caulfield, "Morphology of connective tissue in skeletal muscle," *Tissue and Cell*, vol. 12, no. 1, pp. 197–207, 1980.

[52] J. Hughes, U. Culha, F. Giardina, F. Guenther, A. Rosendo, and F. Iida, "Soft manipulators and grippers: a review," *Frontiers in Robotics and AI*, vol. 3, p. 69, 2016.

[53] V. S. Joseph, T. Calais, T. Stalin, S. Jain, N. K. Thanigaivel, N. D. Sanandiya, and P. V. y Alvarado, "Silicone/epoxy hybrid resins with tunable mechanical and interfacial properties for additive manufacture of soft robots," *Applied Materials Today*, vol. 22, p. 100979, 2021.

[54] L. Gerez, C.-M. Chang, and M. Liarokapis, "Employing pneumatic, telescopic actuators for the development of soft and hybrid robotic grippers," *Frontiers in Robotics and AI*, vol. 7, p. 601274, 2020.

[55] I. Hussain, Z. Iqbal, M. Malvezzi, L. Seneviratne, D. Gan, and D. Prattichizzo, "Modeling and prototyping of a soft prosthetic hand exploiting joint compliance and modularity," in *2018 IEEE International Conference on Robotics and Biomimetics (ROBIO)*. IEEE, 2018, pp. 65–70.

[56] J. Zhou, X. Chen, U. Chang, J.-T. Lu, C. Leung, Y. Chen, Y. Hu, and Z. Wang, "A soft-robotic approach to anthropomorphic robotic hand dexterity," *IEEE Access*, vol. 7, pp. 1–1, 08 2019.

[57] A. Dey, I. Eagle, and N. Yodo, "A review on filament materials for fused filament fabrication," *Journal of Manufacturing and Materials Processing*, vol. 5, p. 69, 06 2021.

[58] M. Egbo, "A fundamental review on composite materials and some of their applications in biomedical engineering," *Journal of King Saud University - Engineering Sciences*, vol. 33, 07 2020.

[59] M. C. Tanzi, S. Farè, and G. Candiani, "Chapter 1 - organization, structure, and properties of materials," in *Foundations of Biomaterials Engineering*, M. C. Tanzi, S. Farè, and G. Candiani, Eds. Academic Press, 2019, pp. 3–103. [Online]. Available: https://www.sciencedirect.com/science/article/pii/B9780081010341000013

[60] M. Ziaee, J. W. Johnson, and M. Yourdkhani, "3d printing of short-carbon-fiber-reinforced thermoset polymer composites via frontal polymerization," *ACS Applied Materials & Interfaces*, vol. 14, no. 14, pp. 16 694–16 702, 2022.

[61] E. Kurkin and V. Sadykova, "Application of short fiber reinforced composite materials multilevel model for design of ultra-light aerospace structures," *Procedia Engineering*, vol. 185, pp. 182–189, 2017, electric Propulsions and Their Application. [Online]. Available: https://www.sciencedirect.com/science/article/pii/S187770581731490X

[62] V. Annamalai, S. Vijayan, H. Saeedipour, and K. Goh, "The rise of short fibre reinforced plastics," *Reinforced Plastics*, vol. 64, no. 2, pp. 97–102, 2020. [Online]. Available: https://www.sciencedirect.com/science/article/pii/S0034361719302656

[63] M. Schouten, G. Wolterink, A. Dijkshoorn, D. Kosmas, S. Stramigioli, and G. Krijnen, "A review of extrusion-based 3d printing for the fabrication of electro-and biomechanical sensors," *IEEE sensors journal*, vol. 21, no. 11, pp. 12 900–12 912, 2020.

Appendix

Printing Parameters for Loom and Path Printing

Finding the most optimize parameters for both loom and path printing were cumbersome and time consuming process that required lots of trials and error. Hence, the important parameters are mentioned here.

Pin printing

In the pin printing, we used 4 different materials that each requires different print speed, retraction speed, printing temperature, and different procedure. In the following table the major parameters are explained

Table 5.1: Pin materials used in weaving process with functionality and limitations of each material

Pin Material	Printing Temp	Bed Temp	Printing Speed	Retraction Speed	Retraction Value	Flow rate	Additional Note
PLA	205°C	55°C	80mm/sec	45mm/sec	8mm	100%	For smaller than 2mm pins the speed should be reduced to 60mm/sec
PVA	200°C	60°C	30mm/sec	40mm/sec	6mm	105%	Filament Dryness is important, The bed should be turn off after 4mm, The pins are brittle
Layfomm	220°C	50°C	10mm/sec	40mm/sec	6mm	110%	Be sure the filament is dry, Thicker base layer
PET	215°C	60°C	60mm/sec	45mm/sec	8mm	105%	Low lateral force tolerance, best for printing in one iteration and not head change.

Path Pritning

For the path printing purpose, through trial and error, we find the following parameters for path printing that provides the best bonding and encapsulation of the fiber inside the thermoplastic matrix.

Extrusion rate: 120%

Printing speed: 100mm/min

Extrusion temperature: 230°

Printing height from the cavity base: 0.7mm